

WHITE PAPER
ON
NUCLEAR ASTROPHYSICS AND LOW ENERGY NUCLEAR PHYSICS
FOR INVESTIGATION ON THE YEREVAN PROTON CYCLOTRON

Preface

In accordance with the decision of the Government of the Republic of Armenia about the organization of the production of radioisotopes for medical purposes, an accelerator of protons (the C18/18 cyclotron) was acquired from the IBA Company and located in a specialized building located on the territory of the A. Alikhanyan National Laboratory (AANL) Foundation (Yerevan Physics Institute). Besides an internal proton beam of 18 MeV energy suited for the medical radioisotope production, the cyclotron also provides an extracted proton beam of up to 17.6 MeV, which is transferred by a special pipe to the experimental hall enabling to carry out experimental investigations of proton-nuclear interactions of astrophysical and low-energy nuclear physics interest, as well as for a wide range of applications. A significant part of these applications are in the field of space, environmental and medical sciences (radioisotope products, dosimetry, radiation therapy, etc.), radiation and protective effects in space, and technology for the activation of transmutation of nuclear waste based on accelerators. A significant contribution to this area is made by systematic studies of proton-induced reactions on some important structural and instrumental materials.

A detailed review of the existing literature showed that there are serious flaws in the field of proton-induced reactions. To meet the new requirements of the growing medical production of radioisotopes, the development of accelerator technology and the need to improve the characteristics of the codes of nuclear models, it is necessary to conduct a systematic study of the activation cross sections of charged particles in various materials, mainly metals. The lack of experimental data makes it impossible to assess the predictive power of a theoretical model. This lack can be, to some extent, complemented by the considered below experiments on the C18/18 cyclotron.

A large fraction of the planned experiments will be based on the induced activation method. The targets irradiated by the proton beam will undergo gamma-spectroscopic measurements with the help of high-purity germanium (HPGe) detectors in the surface and underground laboratories of AANL. The underground laboratory is placed in the Avan salt mine, which is located in precincts of Yerevan, at the depth of 650 meters of water equivalent. It is provided with a corresponding infrastructure and communication system (including, for example, the data transmission from experimental setups, placed there, to the AANL's web page in real time). The excellent background conditions in the underground laboratory allow one to investigate rare nuclear reactions. The short description of the induced activity-based experiments is given in Appendices 1, 2, 3 and 4. The second group is on-line experiments to be realized with the help of dedicated experimental setups under construction. Appendices 5, 6, 7 and 8 are devoted to the short description of on-line experiments with the extracted proton beam.

The third group of the planned works is devoted to the possibility to form neutron beams and use them in investigation of neutron-induced reactions which are considered in Appendices 9 and 10.

Appendix 1

Low energy proton-induced reactions

R.Avetisyan, A.Barseghyan, Yu.Gharibyan, A.Gyurjinyan, I.Kerobyan, H.Mkrtychyan, V.Yaralov

Contributions of equilibrium and pre-equilibrium reaction mechanisms have been investigated using different reaction model calculations. The excitation functions for pre-equilibrium calculations were newly calculated using hybrid model, geometry-dependent hybrid model and cascade-excitation model [1]. It should be noted, that the predictions of various models differ by more than 5 times. The lack of experimental data makes it impossible to assess the predictive power of a theoretical model.

Of particular interest are studies of the excitation functions of reactions on tungsten $^{nat}\text{W}(p,xn)\text{Re}$, gadolinium $^{nat}\text{Gd}(p,xn)\text{Tb}$ and niobium $\text{Nb}(p,xn)\text{Mo}$. As a result of these reactions, products are obtained, widely used both in medicine (^{186g}Re , ^{152}Tb – PET, ^{155}Tb – SPECT, ^{149}Tb – α particle and ^{161}Tb β particle therapy) and in industry (reactor constructions).

Nuclear reaction data are important in the field of basic and applied sciences. Measurement of relative population of isomeric state of the nuclei will provide information on transfer of energy and angular momentum as well as its dependence on various factors.

Information regarding the isomeric ratio and its dependence on the reaction channel will help in planning the production of medical isotopes to select the reaction channel at which the yield of the isotope of interest is higher.

On the proton beam of cyclotron C18/18, it is proposed to study several reactions for the production of isomeric pairs in the energy range $E_p = 10\text{-}18$ MeV, at which experimental data are currently scarce or even absent, for example, $^{124}\text{Sn}(p,n)^{124m,g}\text{Sb}$; $^{nat}\text{Mo}(p,xn)^{93m,g}\text{Tc}$, $^{94m,g}\text{Tc}$, $^{95m,g}\text{Tc}$; $^{nat}\text{Te}(p,xn)^{120m,g}\text{I}$; $^{nat}\text{Sn}(p,pn)^{116m,g}\text{Sb}$; $^{nat}\text{Sn}(p,n)^{118m}\text{Sb}$; $^{nat}\text{Sn}(p,n)^{120}\text{Sb}$; $^{112}\text{Sn}(p,2p)^{111}\text{In}$; $^{nat}\text{Ag}(p,pn)^{106m,g}\text{Ag}$; $^{112}\text{Sn}(p,pn)^{111m}\text{Sn}$; $^{nat}\text{Sn}(p,pn)^{117m}\text{Sn}$.

Some of these reactions are of radiomedical interest (^{124}Sb , ^{111}In , ^{117m}Sn).

The gap in the experimental data can be, to some extent, filled using the proton beam provided by the cyclotron C18/18.

The obtained data will allow one to perform a complex checking of the predictions of various theoretical models comprised in several comprehensive nuclear reaction codes.

Surveying the information of excitation functions for the $^{nat}\text{W}(p,xn)^{181,182m,182g,183,184m,184g,186}\text{Re}$ in energy region up to 18 MeV and yields of the reactions [2-8] has shown that:

- published cross sections have relatively high errors, the excitation functions were measured in not enough details;
- the reported cross sections from different groups often showed unacceptable deviations both in the values of the cross sections and in their energy scales;
- reported calculated and/or measured thick target integral yields have significant differences.

A new data set for the production cross sections of the $^{181,182m,182g,183,184m,184g,186}\text{Re}$ have much importance in several fields, e.g., for the improvement of model calculations, nuclear medicine, thin layer activation process, and trace element analysis.

The study of isomeric cross section ratio for $^{182m,182g}\text{Re}$ and $^{184m,184g}\text{Re}$ isomer pairs gives important information about the nuclear reaction mechanism, particularly the energy and angular momentum transfer during the reaction process.

For the investigated nuclei by the programs TALYS 1.9 [9] and EMPIRE-3.2 [10] the excitation functions were calculated using the different nuclear models.

The well-known stacked-foil activation technique and subsequent gamma spectrometry will be employed to carry out measurements of excitation functions of reactions $^{\text{nat}}\text{W}(p,xn)^{181,182m,182g,183,184m,184g,186}\text{Re}$. The stack will be formed inserting the Al and Cu foils between the W foils. The Cu and the Al foils will be used to monitor the beam intensity and to degrade the beam energy, respectively.

The advantage of the stacked foil method is that one can get a whole excitation function curve in one single irradiation with the off-line study of the all produced nuclides.

The tungsten W has five naturally occurring isotopes. The list of tungsten isotopes and their abundances is presented in the Table 1.

Isotope	Natural abundance, %
^{180}W	0.12
^{182}W	26.50
^{183}W	14.31
^{184}W	30.64
^{186}W	28.43

Table 1. The list of tungsten isotopes and their abundances

Table 2 provides all reaction channels on natural tungsten and thresholds for these reactions, the lifetime of the daughter nuclei, energy and intensity of characteristic lines. For all reactions channels going on the natural W targets the excitation functions were calculated by nuclear reaction programs TALYS 1.9 [8] and EMPIRE 3.2 [9].

The overall thickness (number of foils) of the stack was determined so that it reduces the beam energy to zero at the last foil.

Nuclei	Half-life	Reactions	Threshold, MeV	E_γ , keV	Intensity, (%)
^{181}Re	20 h	$^{182}\text{W}(p,2n)$	10.5	365.57	57.
^{182g}Re	64 h	$^{182}\text{W}(p,n)$	3.58	169.15	11.3
		$^{183}\text{W}(p,2n)$	9.77		
^{182m}Re	12.7 h	$^{182}\text{W}(p,n)$	3.58	470.32	2.
		$^{183}\text{W}(p,2n)$	9.77		
		$^{183}\text{W}(p,n)$	1.35		

^{183}Re	70 d	$^{184}\text{W}(p,2n)$	8.75	162.32	23.3
^{184g}Re	38 d	$^{184}\text{W}(p,n)$	2.27	792.07	37.5
^{184m}Re	169 d	$^{184}\text{W}(p,n)$	2.27	104.73	13.4
^{186}Re	3.72 d	$^{186}\text{W}(p,n)$	1.36	137.16	9.42

Table 2. The list of investigated reactions

The range of protons beam passing through the stack was calculated by using program SRIM/TRIM-2013 [11].

The schematic diagram of stack is shown in Fig. 1.

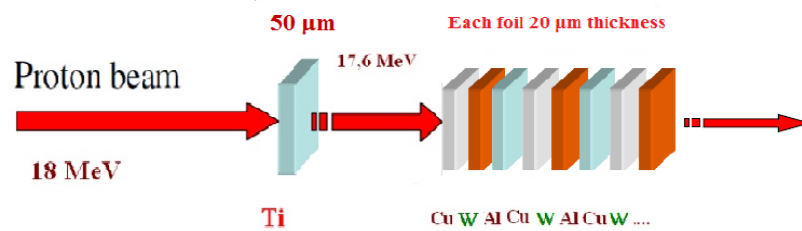


Fig. 1. Schematic arrangement of the stack with Al degrader and Cu monitor foils.

The energy distributions of protons and their standard deviations for the each foil of W determined by Monte-Carlo calculation using program TRIM [11] are shown in Table 3.

The irradiation of target stack will be performed at the external proton beam of the cyclotron C18 at current $1 \mu\text{A}$. Thus, as a result of a single irradiation the excitation function for all of the investigated reactions at 10 values of proton energy from the corresponding threshold of the reaction up to the maximum available energy will be obtained.

Foils, W	Protons energy, MeV
1	16.96 ± 0.165
2	16.00 ± 0.18
3	14.87 ± 0.22
4	13.76 ± 0.273
5	12.71 ± 0.3
6	11.45 ± 0.386
7	10.15 ± 0.53
8	8.77 ± 0.66
9	7.11 ± 0.78
10	5.07 ± 0.97

Table 3. The protons energy in the W foils

The induced gamma activities of the radioisotopes produced from the W foils and the monitor Cu foils will be measured continuously by using gamma-ray spectrometer. The gamma spectrometer is a HPGe (High-Purity Germanium) Coaxial Detector System of type GEM15P4-70. Detector is completed by the DSPEC-LF Digital Gamma-Ray Spectrometer (analyzer) including MAESTRO software.

The experiment will result in the extraction of a large bulk of new experimental data on proton-nucleus interactions, which will be useful for a better understanding of the nuclear structure and the nuclear reactions processes, as well as for testing and improvement of various theoretical models on the low-energy nuclear reactions.

References

1. F. Szelecsényi “Measurement of Cross Sections of Proton Induced Nuclear Reactions on Ti, Ni, Zn, Cd, and Au up to 30 MeV and Their Application in Radioisotope Production” PhD. Thesis, Lajos Kossuth University Debrecen, Hungary 1997.
2. F. Tárkányi, S. Takács et al., *Nuc. Instr. Meth.*, **B 252** (2006), 160-174.
3. X. Zhang, W. Li et al., *Radiochim. Acta*, **86** (1999), 11-16.
4. E. Persico et al., Excitation functions and yields for re-186g production by proton cyclotron irradiation, *Cyclotrons and Their Applications 2007*, Eighteenth International Conference.
5. S. Lapi, W.J. Mills et al., *Appl. Radiat. Isot.*, **65** (2007), 345-349.
6. M.U.Khandaker, M.S,Uddin et al, <http://arvix.org/ftp/nucl-ex/papers/0703/0703035.pdf>.
7. N. C. Schoen, G. Orlov, and R. J. McDonald, Excitation functions for radioactive isotopes produced by proton bombardment of Fe, Co, and W in the energy range from 10 to 60 MeV,*Phys. Rev. Lett.* 112, 068103.
8. R. Michel, A.S.M.F. Choedhury et al., in S.M. Quaim (ed.), *NEA/NSC/DOC(2005)27, ONDC(GER)-0051, Jül-4194, FZJ, 2005*, p. 31.
9. A. Koning, S. Hilaire, S. Goriely, *TALYS-1.9, A nuclear reaction program*, 2017.
10. M. Herman et al., *EMPIRE-3.1 Rivoli modular system for nuclear reaction calculations and nuclear data evaluation*, February 8, 2013.
11. J.F. Ziegler, J.P. Biersack, U. Littmark, *The code of SRIM – the Stopping and Range of Ions in Matter*, January 1, 2000, Version 2000.XX.

Appendix 2

Study of rare and exotic channels of proton-nucleus interactions

A.Aleksanyan, S.Amirkhanyan, H. Gulkanyan, T.Kotanjyan, V.Pogosov, O.Pogosova,
L.Poghosyan

2.1 Study of (p, γ) and (p,n) reactions of astrophysical interest

The stellar nucleosynthesis is a complicated multi-stage process inherent to the evolution of the Universe. One of its prominent characteristics is the abundance of chemical elements and

their isotopes in various cosmic objects. The contemporary astrophysical models are not yet able to describe satisfactorily the abundances for a number of isotopes, in particular, for several isotopes of elements above iron. This concerns, first of all, 35 proton-rich stable nuclei which abundances are by one or two order of magnitude smaller than those for other isotopes of the same element. These isotopes are named ‘avoided’ or p-nuclei. It is established at present [1-3], that stellar nucleosynthesis of comparatively high-abundance isotopes, neighboring to p-nuclei, proceeds through a multi-step chain of consecutive neutron capture (n,γ) and the nuclear β -decay reactions, while in the synthesis of p-nuclei an essential role is played by other, so called p-processes, including first of all the (γ,p) reactions (see [3], as well as the (γ,n), (α,p), (p,γ), (p,n), reactions [3, 4]. Necessary conditions for p-processes can be provided in the explosive nucleosynthesis stages of the evolution of stars and close-binary stellar systems. To simulate as precisely as possible the stellar evolution, one needs a detailed information on a number of key quantities inferred from nuclear physics experiments, such as the nuclear masses, the β -decay half-lives and the cross sections of aforementioned reactions at the energy range corresponding to the stellar temperatures (so called ‘Gamow window’ for energy) [5]. The experimental data on (p,γ) reactions of astrophysical interest were mainly obtained in the last two decades (see references in [3]), using proton beams provided by low-energy proton accelerators at the energy range of a few MeV, being the most important range for the stellar nucleosynthesis of p-nuclei. The most part of these kinds of reactions are not still studied experimentally. The list of these reactions includes more than 150 (p,γ) processes on various isotopes of 45 chemical elements from germanium to mercury (see [3]). Several reactions from this list are suggested to be object of experimental investigations using the proton beam of the cyclotron. The anticipated data will help in simulations of the chemical evolution of the Universe. For the majority of the $A(p,\gamma)B$ type reactions under consideration, it is not mandatory to register the accompanying prompt γ -quanta, but is sufficient to detect ‘delayed’ gammas emitted after the β -decay of the daughter B nucleus (the so called activation method), provided that the intensity of delayed γ -quanta is sufficiently large to be disentangled from the background radiation and that the half-life $T_{1/2}$ of the daughter B nucleus is sufficiently large ($T_{1/2} > 1$ hour) for transportation of targets (irradiated by protons) to the place foreseen for the spectrometric measurements with the help of photodetectors. The data on cross sections of reactions (p,γ) obtained with the activation method at a few MeV energy range of projectile protons are available for the following nuclei: ^{70}Ge [6], ^{74}Se , ^{76}Se [7], ^{84}Sr , ^{86}Sr , ^{87}Sr [8], ^{92}Mo , ^{94}Mo , ^{95}Mo , ^{98}Mo [9], ^{96}Ru , ^{98}Ru , ^{99}Ru , ^{104}Ru [10], ^{102}Pd , ^{104}Pd [11], ^{106}Cd , ^{108}Cd [12], ^{116}Sn [13], ^{126}Te [14], ^{152}Gd [15]. The measurements in the said energy range, including also ‘in-beam’ measurements with registration of prompt γ -quanta, involve around 30 (p,γ) reactions on various targets that composes only about 20% of reactions of astrophysical interest [3]. As for remaining 80% of reactions, the cross sections for some of them can be measured with the activation method. In the first-term measurements at the AANL the following target nuclei will be used: ^{117}Sn , ^{124}Sn , ^{152}Gd , ^{160}Gd , ^{174}Hf , ^{180}W , ^{190}Pt .

Certain contribution to the production of avoided nuclei can be provided by two-step (p,γ) reactions [4]. At the first step, the (p,γ) reaction produces an intermediate radioactive isotope followed by participation of the latter in the next (p,γ) reaction leading to the formation of an avoided nucleus. The list of the first-step (p,γ) reactions is given in [4]. Some of these reactions are assumed to be investigated at the cyclotron C18/18.

Similarly to the consecutive chain of two (p, γ) reactions, the production of avoided nuclei can be also contributed by the consecutive chain of two (p,n) reactions [4]. The list of the first-step (p,n) reactions is given in [4]. Some of these reactions are assumed to be investigated at the cyclotron C18/18.

2.2 Study of proton capture reactions on actinide nuclei

The proton capture reactions, such as the radiation capture reaction (p, γ) and exclusively one or more neutron emission reactions (p,kn), are to date least-explored for nuclei heavier than thorium. In particular, for ^{238}U and ^{239}Pu nuclei the data on (p, γ) reaction are absent at all, while the cross sections of reactions (p,kn) are measured only for ^{238}U at incident energy $E_p = 200$ MeV [16]. We suggest to fill partly this gap in experimental data using proton beams with energies up to $E_p = 17$ MeV at the cyclotron C18/18. The induced activity method and gamma-spectroscopic measurements will be utilized to measure the cross sections of several reactions producing sufficiently long-living beta-radioactive isotopes of neptunium and americium in proton-induced reactions in, respectively, ^{238}U and ^{239}Pu thin targets. The list of radioisotopes under consideration includes (in parentheses the half-lives are quoted): ^{239}Np (2.36 days), ^{238}Np (2.1 days), ^{236}Np (22.5 hours), with the reaction threshold energies up to 13.1 MeV and ^{240}Am (50.8 days), ^{239}Am (11.9 hours), ^{238}Am (98 min), ^{237}Am (73.6 days), with the reaction threshold energies up to 15 MeV. All considered radioisotopes have sufficiently intense gamma-lines to be unambiguously identified.

2.3 Search for tetraneutron in proton-bismuth interactions

The planned investigations include the searching for the tetraneutron in proton-induced reactions on ^{209}Bi , using the BGO ($\text{Bi}_4\text{Ge}_3\text{O}_{12}$) crystals as target which will be irradiated by the proton beam from the C-18 cyclotron. In particular, the ^4n cluster will be searched for in reactions



which, at the mean energy $\langle E_p \rangle \sim 14$ MeV of protons (taking into account ionization losses in the target) can proceed only if the binding energy of the ^4n state exceeds ~ 4 MeV per neutron for the case of the reaction (1) and ~ 3 MeV per neutron for the case of the reaction (2). The reaction (1) will be searched for via the off-line detection of the γ -radiation from ^{205}Bi (with $T_{1/2} = 15.2$ days), namely, by its most intense two lines $E_\gamma = 703.4$ keV ($I_\gamma = 31.1\%$) and 987.8 keV ($I_\gamma = 16\%$), while the reaction (2) will be searched for by the two lines $E_\gamma = 807.4$ keV ($I_\gamma = 21.8\%$) and 1032.3 keV ($I_\gamma = 31.7\%$) of ^{206}Po (with $T_{1/2} = 8.8$ days) and the most intense three lines $E_\gamma = 803.1$ keV ($I_\gamma = 99\%$), 881.0 keV ($I_\gamma = 66.2\%$) and 1718.7 keV ($I_\gamma = 31.9\%$) of ^{206}Bi (with $T_{1/2} = 6.24$ days). Gamma-spectroscopic measurements will be performed in the underground laboratory by the low-background setup on the base of the HPGe detector.

2.4 Search for multineutron bound states in proton-induced fission of thorium

In view of recent experimental results [26, 27], we suggest to extend the investigations aimed at the searching for multineutron bound states ^xn ($x \geq 4$) in induced fission of heavy nuclei. To this end the proton-induced fission of thorium will be considered:

$$p + {}^{232}\text{Th} \rightarrow {}^x\text{n} + X_f, \quad (3)$$

where X_f denotes the undetected fission products of ${}^{232}\text{Th}$. The secondary target method applied in [26, 27] for the detection of the hypothetical ${}^x\text{n}$ nucleus will be used. The induced γ -activity in the secondary (antimony) target will be utilized. A natural antimony target (containing 57.21% of ${}^{121}\text{Sb}$ and 42.79% of ${}^{123}\text{Sb}$) will be used for identification of secondary reactions

$${}^x\text{n}({}^{121}\text{Sb}, {}^{125}\text{Sb})(x-4)\text{n} \quad (4)$$

and/or

$${}^x\text{n}({}^{123}\text{Sb}, {}^{125}\text{Sb})(x-2)\text{n} \quad (5)$$

by means of off-line measurement of the γ -activity of the long-living isotope ${}^{125}\text{Sb}$ (with the half-life $T_{1/2} = 2.78$ years) built-up during a long-term irradiation of the initial thorium target (assuming non-vanishing probability of the reaction (3)). It is suggested to install the secondary target as close as possible to the thorium target, say, at the distance of 5 cm, and at polar angle of about 90° with respect to the proton beam direction. An additional aluminum pill of 1 cm thickness will be placed upstream of the antimony target. It serves, on the one hand, as an absorber for charged fragments of the thorium fission, allowing, in particular, to exclude the contribution from the background reactions such as ${}^6\text{He}({}^{123}\text{Sb}, {}^{125}\text{Sb}){}^4\text{He}$ or ${}^8\text{He}({}^{121}\text{Sb}, {}^{125}\text{Sb}){}^4\text{He}$. On the other hand, it serves as a moderator for a multineutron bound system, slowing down the latter from the energy of about $E \sim 1$ MeV per nucleon to significantly smaller energies, at which the cross sections for exothermic (if the ${}^x\text{n}$ nuclei are weakly bound) reactions (4) and (5) behave as $\sigma \sim (Q/E)^{1/2}$ (Q being the Q -value of the reaction), and can reach rather large values, e.g., about 10^3 b at energies around several keV [27]. After as long as possible exposition the antimony targets will be transported to the underground laboratory and processed with the help of the HPGe detector, searching for gamma-rays associated with the β -decay of ${}^{125}\text{Sb}$ with energies $E_\gamma = 427.9$ keV (29.6%), 463.4 keV (10.5%), 600.6 keV (17.6%) and 635.9 keV (11.2%). The corresponding intensities of gamma-lines are quoted in parentheses.

2.5 Ecological monitoring (including an investigation of Amulsar mine's influence on the water resources)

We suggest applying the proton-induced activation method to analyze the samples taken from groundwater monitoring places. The radioactive nuclei, produced in the proton-induced reactions, such as ${}^{75}\text{As}(p,n){}^{75}\text{Se}$, ${}^{201}\text{Hg}(p,\gamma){}^{202}\text{Tl}$, ${}^{206}\text{Pb}(p,n){}^{206}\text{Bi}$ and so on, will be identified with the help a low-background γ -spectrometer in the underground laboratory of AANL. According to our studies, this method can support higher sensitivity than traditional methods. This will enable a fast detection and analysis of heavy metals and other toxic mixtures in the samples.

References

- [1] G. Wallerstein et al., Rev. Mod. Phys. 69 (1997) 995
- [2] J.J. Cowan, F.-K. Thielemann, J.W. Truran, Phys. Rep. 208 (1991) 267
- [3] T. Rauscher et al., Rep. Phys. Prog. 76 (2013) 066201
- [4] J.W. Truran and A.G.V. Cameron, Astrophys. J. 171 (1972) 89
- [5] T. Rauscher, Phys. Rev. C81 (2010) 045807

- [6] G.G. Kiss et al., Phys. Rev. C76 (2007) 055807
- [7] Gy Gyürky et al., Phys. Rev. C68 (2003) 055803
- [8] Gy Gyürky et al., Phys. Rev. C64 (2001) 065803
- [9] T. Sauter, F. Käppeler, Phys. Rev. C55 (1997) 063127
- [10] J. Bork et al., Phys. Rev. C58 (1997) 010524
- [11] A. Spyron et al., Phys. Rev. C77 (2008) 065801
- [12] N. Özkan et al., Nucl. Phys. A710 (2002) 469
- [13] Gy Gyürky et al., J. Phys. G34 (2007) 817
- [14] R.T. Güray et al., Phys. Rev. C80 (2009) 035804
- [15] R.T. Güray et al., Phys. Rev. C91 (2015) 055809
- [16] www.nndc.bnl.gov
- [17] H. Ogata et al., J. Phys. Soc. Japan **15** (1960) 1719
- [18] H. Ogata et al., J. Phys. Soc. Japan **15** (1960) 1726
- [19] L. Milazzo-Colli et al., Nucl. Phys. A **218** (1974) 274
- [20] R. Bonetti et al., Phys. Rev. C **28** (1983) 1892
- [21] E. Tel et al., Indian J. Phys. **83** (2) (2009) 193
- [22] T. Siiskonen et al., NIM B **267** (2009) 3500
- [23] M. Herman et al., Nuclear Data Sheets **108** (2007) 2655
- [24] [http:// www.talys.eu](http://www.talys.eu)
- [25] [http:// www.nds.iaea.org](http://www.nds.iaea.org)
- [26] B.G. Novatskii et al., JETP Lett. 96, 280 (2012)
- [27] B.G. Novatskii, S.B. Sakuta and D.N. Stepanov, JETP Lett. 98, 656 (2013)

Appendix 3

Study of (p, α), (p,2n), isomeric pair production and transmutation reactions

N.Demekhina (AANL), A.Balabekyan (YSU)

3.1 The (p, α) reactions.

The investigation of the α -production at low energies is of a great interest because allow to determine the role of definite channels in complicated process. The role of different mechanisms depends noticeably on the energy of incident particles. At very low proton energy $E_p < 10$ MeV and comparatively high excitation energy (especially for exothermic reactions) the dominant mechanism of α -emission is the formation of compound nuclei [1]. Direct emission of α -particles begins at energies $E_p \geq 11$ MeV [2]. At higher energies the pre-equilibrium emission of α -particles is manifested (at least for heavy nuclei $A > 100$ [3, 4]). The availability of α -particles, as a cluster inside nucleus was considered as a “performance factor” in different theoretical predictions [5, 6]. The E_p - and A -dependences are not well established yet. As a result the theoretical models fail in describing the experimental data in this energy region [7, 8].

In several works [8, 10] authors pointed, that probability of the α -particles formation in nuclear matter depends on nucleon composition and shell structure. In the project it is supposed to measure α -particles production in the reactions on different isotopes of Ti, Ni.

The yields of the residual nuclei after α -emission will be measured by using activation method, which allows selecting the interaction channel by using spectroscopic properties of the residual nuclei: energies of the gamma transitions (E_γ) and the half-life of the decay products ($T_{1/2}$) [9].

In tabl.1 the targets for irradiation and products, which will be produced in reactions, are presented.

Table 1

Target, reaction	Product	$T_{1/2}$	E_γ (keV)
$^{46}\text{Ti} + \text{p}$	^{43}Sc	3.891h	372(23%)
$^{47}\text{Ti} + \text{p}$	^{44}Sc	3.927h	1157(99.9%)
$^{49}\text{Ti} + \text{p}$	^{46}Sc	3.79d	889.97(99.98%) 1120.54(99.98%)
$^{50}\text{Ti} + \text{p}$	^{47}Sc	3.349d	159.377(68.3%)
$^{58}\text{Ni} + \text{p}$	^{55}Co	17.53h	931(75%)
$^{64}\text{Ni} + \text{p}$	^{61}Co	1.65h	908 (3.6%)
^{116}Sn	^{117}In	2.8d	171(90%), 245.34(94%)
^{120}Te	^{117}Sb	2.8h	158(86%)

The obtained data on cross sections of α -particles production allow performing a checking of the predictions of various models on the alpha cluster formation probability in nuclei.

3.2 The origin of the avoided nuclei.

Accordingly to modern theory of the cosmic nucleosynthesis a group of low abundance (1%-0.1%) stable neutron-deficit nuclei are formed mainly in p-process via (p, γ), (p,n) [10] and (p,2n) [11] reactions. To this group belong neutron-deficit isotopes of following elements : ^{74}Se , ^{78}Kr , ^{84}Sr , $^{92,94}\text{Mo}$, $^{96,98}\text{Ru}$, ^{102}Pd , $^{106,108}\text{Cd}$, 111 , ^{112}Sn , ^{120}Te , ^{124}Xe , $^{130,132}\text{Ba}$, $^{136,138}\text{Ce}$, ^{144}Sm , ^{152}Gd , $^{152,158}\text{Dy}$, $^{162,164}\text{Er}$, ^{168}Yb , ^{174}Hf , ^{184}Os , ^{190}Pt , ^{196}Hg [12].

It was shown that the majority of the avoided nuclei can be obtained in the (p,2n) reactions [11] at proton energies more than 10 MeV .This kind protons may occur in stellar atmosphere due the cold electromagnetic acceleration [11]. The data in this field are very scare [1] and concern only several element formations. This problem opens a wide region for experimental investigations. In present project the activation methods is proposed for measurement the cross sections of the avoided nuclei [9]. However, all these nuclei are stable and (p,2n) reaction cross section can be measured on the neighboring nuclei. In present project we plan the measurements of the cross sections for several reactions (Table 2). Irradiations of the different isotopes allow to obtain the dependence of the probability of (p,2n) reaction on the target nucleon composition.

Table 2

Target	Reaction	Product	T _{1/2}	E _γ (keV)
¹²⁰ Sn	p,2n	¹¹⁹ Sb (¹¹⁹ Te)	(16,03h)	844
¹¹⁸ Sn	p,2n	¹¹⁷ Sb	2.8h	158(86%)
¹⁰⁸ Cd	p,2n	¹⁰⁸ In	58min	242 (41%), 32(100%)
¹¹⁰ Cd	p,n	¹¹⁰ In	4.9h	657(98%)
¹²² Te	p,2n	¹²¹ I	2.12h	212(84%)
¹²⁴ Te	p,2n	¹²³ I	13.27h	158(83%)
¹²⁵ Te	p,2n	¹²⁴ I	4.17d	602.729(63%)

3.3 Isomeric ratio measurements.

One of the main factors affecting on the formation of the isomeric state are the nucleon composition and the shell structure of the target and produced nuclei [13]. The influence of the nuclear properties on high spin state formation in low energy range can appear more distinctly [13]. In present work will be studied the effect of the target isotopic composition in simple (p,n) and (p,γ) reactions. The Cd isotopes should be used as targets and the activation analysis will be employed to distinguish of residuals in the different spin states [9]. In Tabl.3 are listed the proposed targets and reaction products. The measured cross sections will be compared with available data at higher energies as well as the predictions of various theoretical models.

Table 3

Target	Reaction	Product	Spin	T _{1/2}	E _γ , keV(%)
¹⁰⁸ Cd (0+)	p, n	^{108m} In	2+	39.6min	1529(7.3) 1986.96(12.4)
		^{108g} In	7+	58min	1032(35) 1056(29) 1299(15.1)
¹⁰⁸ Cd	p, γ	¹⁰⁹ In	9/2+	4.2h	203.5(74)
¹¹¹ Cd (1/2+)	p, γ	^{112m} In	4+	20.56min	156 (132)
		^{112g} In	1+	14.97min	617(4.6)
¹¹⁴ Cd (0+)	p, n	^{114m} In	1/2+	44.86h	3362(45)
	p, γ	^{115m} In	5+	49.5d	190.3(15.56)
¹¹⁶ Cd (0+)	p, γ	^{117g} In	9/2+	43min	158.56 (87) 553(100)
		^{117m} In	1/2+	116.2min	315.3(19)

3.4 Investigation of the possibility for transmutation of selected long-lived isotopes present in the radioactive waste of NPP.

The aim is to study nuclear processes and to assess the yields of different reaction products of long-lived radioactive waste transmutation. In this connection, it is planned to irradiate selected radioactive-containing samples (or neighboring elements) on proton beams and by using induced activity method to make the analysis of the reaction cross sections and compare the data with the model predictions.

Investigation of the proton-nucleus interactions will allow to assess the possibility for transmutation of certain radioactive products of the processes accompanied by emission of a few nucleons, such as (p, n) and (p, pn). This type of reactions proceeding both by forming compound nuclei and also via direct interaction have significant cross-sections of ~50-100 mb in the projectile energy range of 10-15 MeV. Similar data were obtained on the isotopes $^{77,80}\text{Se}$ and ^{88}Sr in the (p, n) reaction [14, 15] and in the model predictions [16].

Table 4

Long lived isotope	Half life	Investigated reaction	Rad. residuals	Half life	γ -energy (keV)	Intensity (%)
^{79}Se	$1.13 \cdot 10^6$ y	^{77}Se (p, n)	^{77}Br	65h	238.9	23
					297.2	16
					520	22
^{90}Sr	28.5 y	^{88}Sr (p, n)	^{88}Y	106.65 d	898	93.7
					1836	99
$^{99\text{g}}\text{Tc}$	$2.111 \cdot 10^6$ y	^{99}Ru (p, n)	^{100}Rh	20.8h	539	80.6
					822	21.09
					1107	13.6

The published experimental results on these reactions on ^{90}Sr and ^{79}Se isotopes (with the value of the Coulomb barrier ~ 8 MeV) confirm the maximum cross section at proton energy range 10-13 MeV. It is planned to make some test measurements on stable isotopes which are the closest to the radioactive nuclei ^{79}Se and ^{90}Sr , and to assess the possibility of transmutation of radioactive isotopes in such processes (Table 4). The obtained data will allow to verify the results of the measurements and to choose the necessary energy range. For the transmutation of ^{99}Tc ($T_{1/2} = 2.111 \cdot 10^5$ y), being formed in the production of radiopharmaceuticals, one can use

(p,n) reaction followed by the creation of ^{100}Ru isotope. As ^{100}Ru isotope is stable and not measurable by induced activity method, similar reaction yield can be investigated in the (p,n) process on ^{99}Ru (or $^{\text{nat}}\text{Ru}$) target (the Q-values of these two reactions are positive).

References

1. <http://www.bnl.gov>
2. H.Ogata et al Phys.Soc.Japan 15,1726,1960
3. I.Milazzo-Colli et al Nucl.Phys. A 218,274,1974
4. R.Bonetti et al Phys.Rev.C28, 1892,1983
5. E.Tel et al Indian JPhys.83,193,2009
6. T.Siskonen et al. NIM B267,3500,2009
7. A.Chevarter et al Phys.Rev.C11,886,1975
8. Dong Bai et al. arXiv:1809.04952v1[nucl-th]13Sep 2018
9. G.S. Karapetyan Eur. Phys. J. Plus 130 (9), 180,2015
10. J.W.Truran and A.G.V.Cameron Astrophus.J.171,89,1972
11. D.A.Frank-Kamenecckij Soviet .Physics Uspekhi 68,529,1959
12. Zs. Fulop et al Nucl.Phys.A758,90c-97c,2005
13. S.A.Karamian Preprint JINR E-15-2012-65
14. Appl.Radiat. Isot. 60.899.2004
15. Appl.Radiat. Isot 67,1320,2009
16. <http://dnr080.jinr.ru/lise/>

Appendix 4

Application of thin layer activation technique for surface wears studies

by charged particle induced nuclear reactions

R.Avetisyan, A.Barseghyan, Yu.Gharibyan, A.Gyurjinyan, I.Kerobyan, H.Mkrtchyan, V.Yaralov

Wear and corrosion lead to the destruction of materials from the surface of metallic and non-metallic components. The reliability of industrial equipment, transport systems and other machine parts is highly dependent on wear. The need for appropriate equipment for monitoring wear is determined by three main factors: economy, safety and energy conservation. Depreciation may endanger not only the safety of the operating equipment, but also staff. In many cyclotron laboratories the accelerator is partly used for industrial applications. One of them is the so called TLA (Thin Layer Activation) which is mainly used for wear (corrosion, erosion etc.) measurements.

The use of cyclotron beams for the study of materials covers a wide range of issues from analytical studies to radiation damage, material modification and solid state physics. Currently, the use of particle beams of cyclotrons in materials research is steadily growing. These studies are carried out in the following areas:

1. Determination of material composition, impurities and depth distribution of unwanted impurities or atoms;
2. The study of radiation damage to materials in order to understand the mechanism of damage;
3. Definition of methods for the development of materials with the best radiation properties;
4. The use of particle beams to find ways to improve the existing properties of the investigated material.

To conduct these studies, the TLA method is widely used [1]. The method TLA is a powerful nuclear method. It is based on the production of a radioisotope on the surface of a material as a result of a nuclear reaction caused by charged particles, followed by an estimate of the loss of activity, which is a measure of the loss of materials ranging from nanometers to hundreds of micrometers in the areas of wear, corrosion or erosion. Wear causes enormous financial and environmental damage in various fields of activity. For example, the automotive industry spends enormous resources every year to minimize wear and tear on automobile engines. To this end, research is being conducted aimed at reducing the rate of wear. These studies need to be developed in methods and technologies to obtain specific data in tribology (a field of science that studies abrasion and wear). From a nuclear technology point of view, TLA has several advantages.

In developed and developing countries, the TLA method is widely used in industrial research and development. This method helps to increase the service life and reliability of various machines, plants and processes [2]. At the same time, the results obtained, for example, in the automotive industry, allow us to design and manufacture vehicles with low fuel consumption. This method is now in use in the automobile industry in Germany, the United States, Great Britain and Japan [3]. At VEC in Calcutta studies by TLA method for motor parts have been performed also [4].

The principle basis of TLA is the creation of an appropriate radionuclide in a given material at a well-defined depth over a selected area. This activation is achieved by cyclotron accelerator through nuclear reactions induced by charged particles such as protons, deuterons, alphas and ^3He . Activation with charge of few mC is in generally enough to reach the activity needed for TLA applications [5].

The obtained isotopes and their half-life are shown in Table I [6].

Table 1. The recommended list of produced isotopes

Element	Beam	Isotope	Half-life
Be	^3He	^7Be	53.3 d
C	^3He	^7Be	53.3 d
Mg	d	^{22}Na	2.62 y
Al	???	^{22}Na	2.62 y
Si	d	^{22}Na	2.62 y
Ti	p	^{48}V	16.0 d

V	d	^{51}Cr	27.7 d
Cr	p	$^{52}\text{Mn}, ^{54}\text{Mn}$	5.7 d, 312.3 d
Mn	p	^{54}Mn	312.3 d
Fe	p	^{56}Co	78.5 d
Co	p	^{58}Co	70.8 d
Ni	d	$^{58}\text{Co} + ^{56}\text{Co}$	
Cu	p	^{65}Zn	244.1 d
Zn	d	^{65}Zn	244.1 d
Zr	p	$^{92\text{m}}\text{Nb}$	10.1 d
Nb	p	$^{92\text{m}}\text{Nb}, ^{95\text{m}}\text{Tc}$	10.1 d, 61 d
Mo	p	$^{95\text{m}}\text{Tc}$	61 d
Sn	d	^{124}Sb	60.2 d
W	p	$^{184\text{g}}\text{Re}$	38 d

For effective measurement of wear by the TLA method the following conditions must be met [6]:

- Large production cross-section in the given energy range and bombarding particle;
- Half-life should be appropriate to perform the measurement (e.g. by corrosion measurement it could be even months) and short enough to make available a cost-effective radioactive waste handling;
- Gamma energy of the chosen isotope should be large enough to penetrate the wall and shielding of the given machine, because one of the most important advantages of the radioactive wear measurement is that the whole wear study can be performed on running machine/system without disassembling the investigated parts of the system;
- High gamma abundance

Given these requirements the most suitable nuclear reactions that can be induced on basically-used machine construction metals (Fe, Cr, Cu, Zn, Ti, V and Mo) by C18/18 Cyclotron's medium energy beams are tabulated and in Table 2.

Table 2. The composition materials, suitable for investigation on proton beam cyclotron C18/18

Isotope	Reaction	Max x- section, mb at MeV	γ -ray	
			Energy, keV	Abundance, %
^{48}V	$^{48}\text{Ti}(p,n)$	605 at 13	983.525	99.98
^{52}Mn	$^{52}\text{Cr}(p,n)$	122 at 14	935.544	94.5
^{54}Mn	$^{54}\text{Cr}(p,n)$	795 at 11	834.848	99.976
^{54}Mn	$^{54}\text{Mn}(p,p^{\prime})$	409 at 12	834.848	99.976
^{56}Co	$^{56}\text{Fe}(p,n)$	383 at 12	846.77	99.94
^{58}Co	$^{58}\text{Fe}(p,n)$	576 at 11	810.759	99.45
^{65}Zn	$^{65}\text{Cu}(p,n)$	658 at 10	1115.539	50.04
$^{95\text{m}}\text{Tc}$	$^{96}\text{Mo}(p,n)$	231 at 15	835.149	26.6

When an ion beams with appropriate energy impinges on the surface of the sample material, it produces radioactive isotopes. As a result, a thin layer of activity is produced on the surface to a certain depth in the micrometer range. Depth of activation can be controlled by energy ion beam. Wear on activated component will be accompanied by a loss of γ -activity from

the activated site. This loss is measured using a γ -spectrometer using HPGe detector. The quantitative loss of material from the surface can be obtained by comparing the test sample with an appropriate calibration curve [7].

The calibration curve for the measurement of surface loss of material activity during wear, corrosion or erosion can be obtained by stacked-foil activation using standard thin foils of metals.

Laboratory studies of wear are carried out on a double-disc Amsler-type tribometer [8], in which two identical disk gears are mounted on shafts located one above the other. This is the standard type of tribometer in which the gear contact can be simulated in real time to measure wear and friction. In the wear test, two discs rotate against each other on their cylindrical surfaces in the opposite direction with a contact width of 10 mm.

It is proposed to create a multifunctional laboratory bench for studying the wear of machine parts subjected to both translational and rotational motion. The activation of machine parts will be carried out on the extracted proton beam of the cyclotron, and the calibration curves will be calculated using codes TALYS 1.9 [9] and TLA2017 [10].

The result of calculation the specific activity by program TLA2017 [10] of the main radionuclide in depth at EOB produced in the reaction $^{nat}\text{Cu}(p,x)^{65}\text{Zn}$ is shown on Fig. 1.

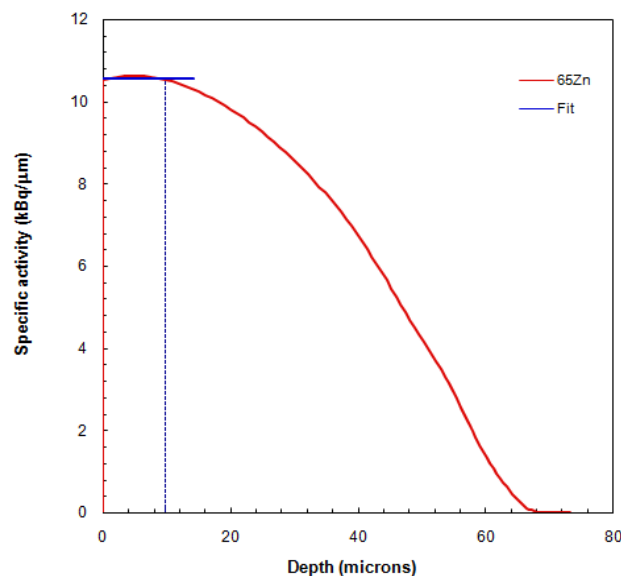


Fig. 1. Specific activity of the main radionuclide in depth at EOB produced in the reaction $^{nat}\text{Cu}(p,x)^{65}\text{Zn}$

The most promising areas for TLA applications are as follows [6]:

- Automobile and engine industry
- Pumps
- Turbines
- Refrigeration systems
- Printing machines
- Textile machinery
- Railway

- Chemical industry
- Oil industry
- Machinery
- Other

References

1. The thin layer activation method and its applications in industry, IAEA-TECDOC-924, IAEA, January 1997.
2. F. Ditroi, S. Takacs et al. "Thin layer activation of large areas for wear study" *Wear* 261 (2006) 1397–1400.
3. Tazawa, S. and Kataoka, S. • "Light Element Analysis of Semiconductors through CPAA and Radio-Nuclide Technique for Machine Wear." in Proceedings of the 1st workshop on Beam Engineering of Advanced Materials. Tokyo, Nov. (1990).
4. Choudhury, D. P., Choudhury, J., Raju, V.S. • Das, S.K., Bhattacharjee, B.B. and Gangadharan, S., "Study of wear between piston ring and cylinder housing of an internal combustion engine by thin layer activation technique," *Nucl. Instr. and Meth. B42*, 375 (1989)
5. D. P. Chowdhury, J. Datta and A. V. R. Reddy "Applications of thin layer activation technique for the measurement of surface loss of materials: an Indian perspective" *Radiochim. Acta* 100, 139–145 (2012).
6. F. Ditrói, S. Takacs, F. Tárkányi, et al. "Application of small energy cyclotrons for thin layer activation technique" Proceedings of the 15th International Conference on Cyclotrons and their Applications, Caen, France.
7. F. Ditrói, S. Takacs, F. Tárkányi, et al. "Nuclear data measurement and compilation for thin layer activation" International Conference on Nuclear Data for Science and Technology 2007.
8. Michel de A. Franca, Julio C. Suita and Cesar M. Salgado "Development of counting system for wear measurements using thin layer activation and the wearing apparatus" 2017 International Nuclear Atlantic Conference - INAC 2017, Belo Horizonte, MG, Brazil, October 22-27, 2017.
9. A. Koning, S. Hilaire, S. Goriely "TALYS 1.9. A nuclear reaction program" (2017).
10. <https://www-nds.iaea.org/tla/>

Appendix 5

Nuclear Astrophysics and Microscopic Clustering in Nuclei opportunities in AANL cyclotron

S. Abrahamyan, R. Ayvazyan, N. Demekhina, H. Elbakyan, N. Grigoryan, V.G.Gurzadyan*
 H. Jilavyan, V. Kakoyan, P. Khachatryan, V. Khachatryan, A.Margaryan*, S.Mirzoyan, H. Vardanyan, S. Zhamkochyan

*contact persons

The Hoyle like states in ^{16}O excited by 18 MeV proton beam and other relevant processes being of particular importance for the stellar evolution, stellar nucleosynthesis and supernovae explosions are proposed to study on the cyclotron. Namely, the Hoyle state in ^{12}C has been established as a possible dilute gas state of three α -particles held together only by the Coulomb barrier, where the three alpha particles are condensed in 0S-orbital state. Identification of α -cluster states analogous to the ^{12}C Hoyle state in heavier α -conjugate nuclei can provide tests of the existence of α condensates in nuclei. Such states are predicted for ^{16}O , ^{20}Ne , ^{24}Mg , ^{28}Si , etc., at excitation energies slightly above the multi- α -particle decay threshold but have not yet been experimentally identified. We propose to carry out a study of the Hoyle-like states of ^{12}C , ^{16}O and ^{20}Ne nuclei by using $p + ^{11}\text{B} \rightarrow ^{12}\text{C}^*$, $p + ^{12}\text{C} \rightarrow ^{12}\text{C}^* + p$, $p + ^{13}\text{C} \rightarrow ^{12}\text{C}^* + d$, $p + ^{16}\text{O} \rightarrow ^{16}\text{O}^* + p$ and $p + ^{19}\text{F} \rightarrow ^{20}\text{Ne}^*$ reactions and of a recently developed active target technique on a 18 MeV proton beam.

Triple α reactions resulting in the synthesis of ^{12}C , which itself participates in the synthesis of the heavier elements in stars, outlines the key role of α particle collisions with 2α resonant state triple α reactions [1-7]. Thus, the triple α reaction plays a crucial role in the nucleosynthesis in the universe. In the triple α reaction, α particle collides with a 2α resonant state, and consequently, excited states of ^{12}C are produced as 3α resonant states. The excited ^{12}C mostly decays to 3α , while a tiny decays to ground state ^{12}C along with the emission of γ -rays.

The α -cluster structure of nuclei with an equal number of protons and neutrons (α -conjugate nuclei) was categorized in 1968 by Ikeda [8] to explain some excited states not reproduced by the shell model. The so called Ikeda diagram schematically is displayed in Fig. 1.

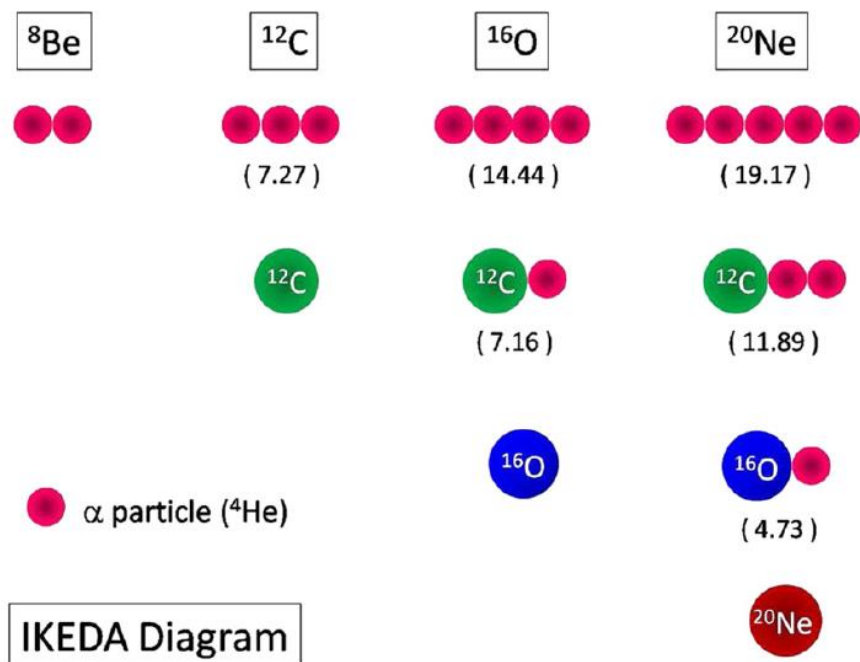


Fig. 1: Schematic of the Ikeda diagram.

Since then, many studies have been performed, but α -clustering is still not completely understood, especially in the medium-light and heavy systems. In the past ten years, a lot of theoretical effort has been focused on the study of 0^+ states built on α -particle cores in self-conjugate nuclei at excitation energies slightly above the multi- α -particle decay threshold. Those states are described as diluted gases of α particles occupying the same 0^+ orbital. They are characterized by a larger radius compared to the normal bound states so that the interaction between α particles is reduced. Therefore, these states can be considered as the best candidates for Bose-Einstein condensates of α particles in the atomic nucleus. Examples of such states are the ground state of ^8Be and the famous ^{12}C Hoyle state. Analogous states are predicted for ^{16}O , ^{20}Ne , ^{24}Mg , ^{28}Si , etc., at excitation energies slightly above the multi- α -particle decay threshold but have not yet been experimentally identified [9,10]. Yamada *et al.* [11] estimated a maximum limit of 10 α particles (^{40}Ca) for such states, resulting from the competition of the short-range attractive force between α particles and the Coulomb repulsion as the number of α particles and the radius of the system increase. Proving the existence of α -cluster states analogous to the ^{12}C Hoyle state in heavier α -conjugate nuclei can provide a way to prove the existence of α condensates in nuclear matter. Kokalova et al. suggest that the signature for multi- α condensed states would be the decay of the excited system into pieces that are themselves condensates, i.e., ^8Be s, ^{12}C Hoyle, etc. [12]. Recently experimental progress has been made on understanding the structure of the ^{12}C Hoyle state [13–19] through the observation of the 2^+ state in the Hoyle-state rotational band [20]. Some experimental work has been performed on heavier systems.

Funaki et al. [20] predicted a 0^+ state in ^{16}O at 15.1 MeV (the 0^{+6} state) with a ^{12}C “Hoyle” state structure coupled to an α particle. Excited states in ^{16}O above the four α -decay threshold have been studied by several authors [21–24]. Few studies exist on ^{20}Ne [25] or ^{24}Mg [26, 27].

An active target has been developed for studying the Hoyle-like states [28]. It is a position and time sensitive detector system based on the Low-Pressure Multi-Wire Proportional Chamber (LPMWPC) technique and Si detectors. The few Torr pressure of hexane (C_6H_{14}), methyl ((OCH₃)₂CH₂) and carbon tetrafluoride (CF_4) serves as a working gas for the LPMWPC, and the ^{12}C , ^{16}O and ^{19}F atoms of these molecules serve as experimental targets. The main advantage of this new target-detector system is its high sensitivity to the low-energy and highly ionizing particles produced at the decay of the Hoyle states of ^{12}C , ^{16}O , and ^{20}Ne nuclei. The threshold energy for detection of α particles and ^{12}C nuclei is about 50 keV and 100 keV, respectively. The time and position resolution of the LPMWPC for ~ 5 MeV alpha particles are approximately 410 ps and 1.5 mm, respectively. The detector system has a modular structure. Each of the four modules consists of two LPMWPC units and one solid-state detector, which allows measuring the trajectories, velocities and energies of low-energy highly-ionizing particles, such as alpha particles and ^{12}C nuclei. The active area of the LPMWPC system and the solid-state detector is $30 \times 30 \text{ mm}^2$. The active target schematically displayed in Fig. 2.

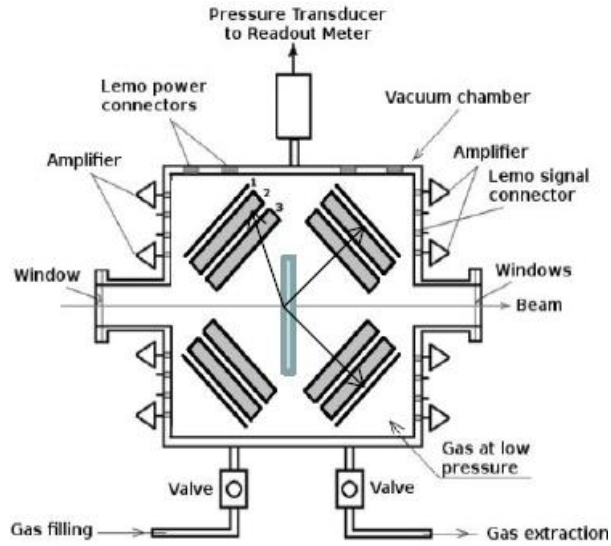


Fig. 2: Schematic of the active target.

We are planning to use this active-target technique to study the Hoyle-like states in ^{12}C , ^{16}O and ^{20}Ne nuclei based on the $p + ^{11}\text{B} \rightarrow ^{12}\text{C}^*$, $p + ^{12}\text{C} \rightarrow ^{12}\text{C}^* + p$, $p + ^{13}\text{C} \rightarrow ^{12}\text{C}^* + d$, $p + ^{16}\text{O} \rightarrow ^{16}\text{O}^* + p$ and $p + ^{19}\text{F} \rightarrow ^{20}\text{Ne}^*$ reactions.

^{12}C nuclei are synthesized by the triple α reaction in the universe. Since heavier elements are synthesized via ^{12}C , the triple α reaction plays a crucial role in the nucleosynthesis in the universe. In the triple α reaction, α particle collides with a 2α resonant state, and consequently, excited states of ^{12}C are produced as 3α resonant states. After that, most of these excited ^{12}C nuclei decay back into 3α , but a tiny fraction of these excited ^{12}C nuclei decays into the ground state of ^{12}C by emitting γ -rays. Therefore, γ -decay probabilities are the key parameters in the ^{12}C synthesis. For example, the γ -decay probability of the Hoyle state (the 0^{+2} state at $E_x = 7.65$ MeV) is known as $4.4(1) \times 10^{-4}$, and the triple α process proceeds via this state at the normal stellar temperature. However, at high temperatures of $T > 10^9$ K, the contribution of the highly excited 3α resonant states such as the 3^{-1} state at $E_x = 9.64$ MeV and the 2_2^{+} state at $E_x = 9.84$ MeV becomes important. Unfortunately, the γ -decay probabilities of these states are still unknown, and it causes uncertainty to calculate the triple α reaction rate. So, we have planned to determine the γ -decay probability of the 3^{-1} state based on the $p + ^{13}\text{C} \rightarrow ^{12}\text{C}^* + d$ reaction and by detecting deuterons in coincidence of α -particles or ^{12}C nuclei after the 3α or γ -decay of $^{12}\text{C}^*$ nuclei. In this way, the γ -decay event can be identified without detecting the γ -rays, and the Γ_γ/Γ decay probability can be obtained from the ratio of the number of all the inelastic events to the number of the γ -decay events. The energy of excitation of $^{12}\text{C}^*$ is determined by the energy and angle of the scattered deuteron and recoiled ^{12}C nucleus.

References

1. Weischer M., Gorres J., Uberseder E., Imbriani G., Pignatari M., Ann. Rev. Nucl. Part. Sci.,60, 381 (2010)
2. Weischer M., Kappeler F., Langanke K, Ann. Rev. Nucl. Part. Sci.,50, 165 (2012)
3. D. Schurmann et al, Phys. Lett. B711, 35 (2012)

4. M Itoh et al, J. Phys: Conf. Series 863, 012019 (2017)
5. V. Liccardo, M. Malheiro, M. S. Hussein, B. V. Carlson, T. Frederico, Nuclear processes in Astrophysics: Recent progress, arXiv:1805.10183 (2018)
6. C. Brogгинi, et al, Experimental nuclear astrophysics in Italy, arXiv:1902.05262, (2019)
7. F. Cuda, Astrophysical Nuclear Reactions: from Hydrogen Burning to Supernovae Explosions, (dissertation, University of Central Lancashire, UK) arXiv: 1806.11179 (2018)
8. K. Ikeda, N. Takigawa, and H. Horiuchi, Prog. Theor. Phys. Suppl. **E68**, 464 (1968).
9. A. Tohsaki, H. Horiuchi, P. Schuck, and G. Ropke, Phys. Rev. Lett. **87**, 192501 (2001).
10. N. Itagaki et al, Phys. Rev. C **75**, 037303 (2007).
11. T. Yamada and P. Schuck, Phys. Rev. C **69**, 024309 (2004).
12. Tz. Kokalova et al., Phys. Rev. Lett. **96**, 192502 (2006).
13. M. Itoh *et al.*, Nucl. Phys. A **738**, 268 (2004).
14. M. Freer *et al.*, Phys. Rev. C **83**, 034314 (2011).
15. M. Freer et al., Rev. Mod. Phys., V. 90, Issue 3, 035004 (2018).
16. M. Itoh *et al.*, Phys. Rev. C **84**, 054308 (2011).
17. W. R. Zimmerman *et al.*, Phys. Rev. Lett. **110**, 152502 (2014).
18. O. S. Kirsebom *et al.*, Phys. Rev. C **81**, 064313 (2010).
19. D. J. Marin-Lambarri et al., Phys. Rev. Lett. **113**, 012502 (2014).
20. Y. Funaki et al., Phys. Rev. Lett. **101**, 082502 (2008).
21. P. Chevallier *et al.*, Phys. Rev. **160**, 827 (1967).
22. M. Freer *et al.*, Phys. Rev. C **51**, 1682 (1995).

Appendix 6

Ternary Fission Studies at 15 MeV Proton Beam

S. Abrahamyan, R. Ayvazyan, N. Demekhina, H. Elbakyan, N. Grigoryan, H. Jilavyan, V. Kakoyan, P. Khachatryan, V. Khachatryan, H. Vardanyan, S. Zhamkochyan, A. Margaryan

The collinear cluster decay in $^{252}\text{Cf}(\text{sf},\text{fff})$, with three cluster fragments of different masses (e.g. ^{132}Sn , $^{52-48}\text{Ca}$, $^{68-72}\text{Ni}$, $Z = 98 \rightarrow Z_i = 50, 20, 28$), observed by the FOBOS group in JINR, has established a new decay mode of heavy nuclei, the collinear cluster tripartition(CCT). The same type of ternary fission has been observed in the reaction $^{235}\text{U}(\text{n}_{\text{th}},\text{fff})$. From these experiments an overall yield of $4 \cdot 10^{-3}/(\text{binary fission})$, has been observed. The data obtained in these experiments also established a CCT decay mode of the same systems into three nuclei of almost equal size (e.g. $Z = 98 \rightarrow Z_i = 32, 34, 32$). The yields of such a decays are a few $1.0 \cdot 10^{-6}/(\text{binary fission})$. Meanwhile, an experiment to detect three heavy fragments large (90°) angles gave a negative result with an upper limit of $1.0 \cdot 10^{-8}/(\text{binary fission})$. We propose an experimental program for a detailed study of the above mentioned TFFF process with the help of the low-pressure MWPC based, large acceptance fission fragment detectors, developed at AANL and 15 MeV proton beam in $p + ^{235}\text{U}$, $p + ^{238}\text{U}$ and $p + ^{239}\text{Pu}$ interactions.

Binary fission has been studied intensively over the last four decades. For an overview there is the book edited by C. Wagemans: The Nuclear Fission Process [1], covering all

important aspects of this process. A more recent theoretical coverage is available as a textbook by H. Krappe and Kr. Pomorski in Ref. [2]. Ternary fission, or light particle accompanied binary fission, has also been studied extensively. The name “ternary” fission has been used so far for such decays, when a third light particle is emitted perpendicular to the binary fission axis [3, 4]. Recent experimental observations and numerous theoretical predictions [5–7, 9] suggest, however, that in ternary decay the collinear configuration is preferred relative to the oblate configuration for heavy systems and ternary fragments with larger charge. The various manifestations of this ternary decay mode and clustering effects studied in the recent years are now referred to as “true ternary fission”, see, e.g., Refs. [10-12]. This new decay mode has been observed for the spontaneous decay of $^{252}\text{Cf}(\text{sf},\text{fff})$ and for neutron induced fission in $^{235}\text{U}(\text{n}_{\text{th}},\text{fff})$, see Refs. [13–15]. Here typical fragments are isotopes (clusters, nuclei with closed shells) of Sn, Ni, and Ca. This new exotic decay can be understood as the breakup of very elongated hyper-deformed shapes, see Ref. [16] for a discussion of hyper-deformation in ^{236}U . The decay is considered with two sequential neck ruptures [15,17] (see Fig. 1). From the experiments reported in Refs. [13, 14] on CCT for $^{252}\text{Cf}(\text{sf}, \text{fff})$ and $^{235}\text{U}(\text{n}_{\text{th}},\text{fff})$ an overall yield of $4 \cdot 10^{-3}/(\text{binary fission})$ has been observed.

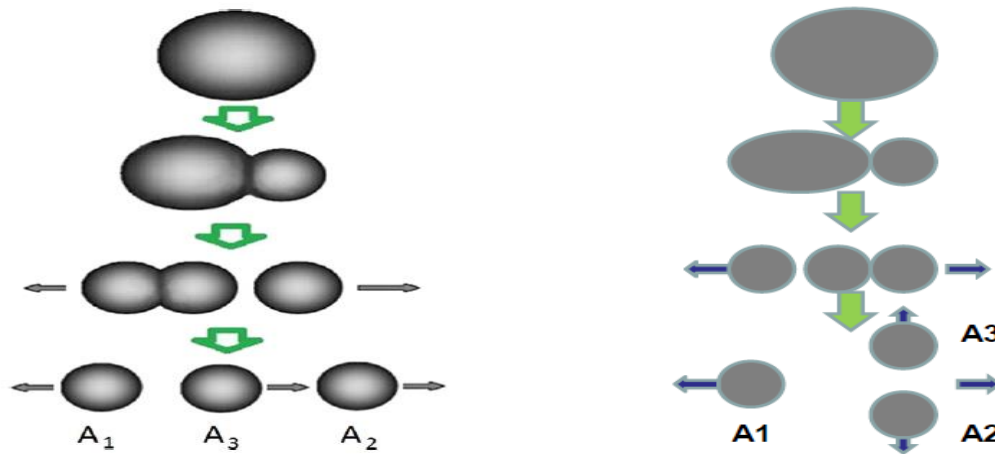


Fig. 1. Schematic of the ternary fission modes. Left side: the collinear cluster tripartition; Right side: tripartition into three fragments produced at large ($\sim 90^\circ$) angles.

The data obtained in these experiments also established a CCT decay mode of the same systems into three nuclei of almost equal size (e.g. $Z=98 \rightarrow Z_i=32, 34, 32$). The yields of such a decays are a few $1.0 \cdot 10^{-6}/(\text{binary fission})$ [18].

Meanwhile, an experiment to detect true ternary fission with three heavier fragments using detectors covering large (90°) angles to detect a triangular shape of the decay-vectors by Schall et al. [19] gave a negative result with a upper limit of $1.0 \cdot 10^{-8}/(\text{binary fission})$.

We propose an experimental program for a detailed study of the above mentioned TFFF process with the help of the low-pressure MWPC based, large acceptance fission fragment detectors, developed at AANL [20-22] and 15 MeV proton beam in $p + ^{235}\text{U}$, $p + ^{238}\text{U}$ and $p + ^{239}\text{Pu}$ interactions. Schematic of the experimental setup is displayed in Fig. 2. Time and position resolution of fission fragments are 150 ps and 350 μm , respectively. By using solid state detectors, masses of fragments can be determined with an accuracy of few nucleons mass.

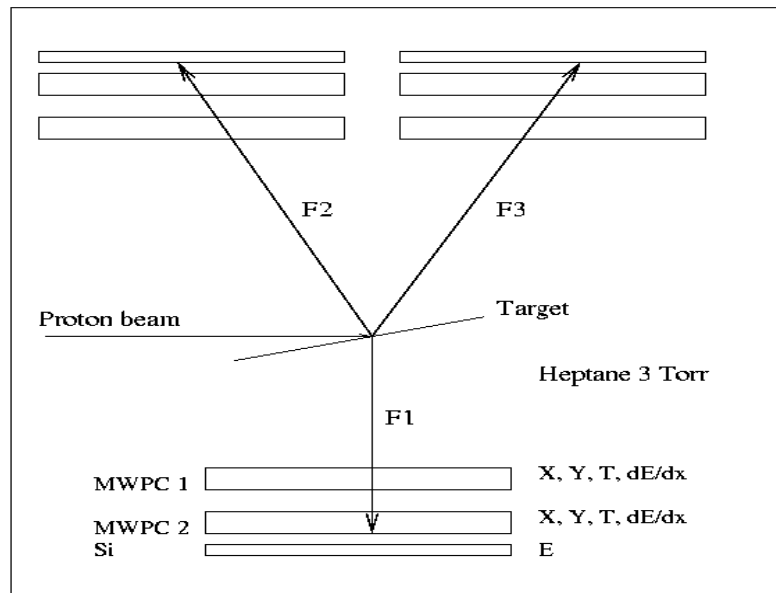


Fig. 2. Schematic of the ternary fission experimental setup.

References

1. C. Wagemans (Ed.), *The Nuclear Fission Process*, CRC Press Inc., 1991.
2. H. Krappe, Kr. Pomorski, *Theory of Nuclear Fission: A Textbook*, Lect. Notes Phys., vol. 838, Springer-Verlag, Heidelberg, 2012.
3. F. Gönnerwein, *Nucl. Phys. A* 734 (2004) 213.
4. F. Gönnerwein, *Europhys. News* 36 (1) (2005) 11.
5. H. Diehl, W. Greiner, *Nucl. Phys. A* 229 (1974) 29.
6. D.N. Poenaru, R.A. Gherghescu, W. Greiner, *Nucl. Phys. A* 747 (2005) 182–205.
7. G. Royer, *J. Phys. G, Nucl. Part. Phys.* 21 (1995) 249.
8. P. Moeller, J.R. Nix, W.D. Meyers, W.J. Swiatecki, *At. Data Nucl. Data Tables* 59 (1995) 185.
9. K. Manimaran, et al., *Phys. Rev. C* 83 (2011), 034609.
10. V.I. Zagrebaev, A.V. Karpov, W. Greiner, *Phys. Rev. C* 81 (2010), 044608; Also V. Zagrebaev, W. Greiner, in: C. Beck (Ed.), *Clusters in Nuclei*, vol. 1, in: *Lect. Notes Phys.*, vol. 818, Springer-Verlag, Heidelberg, Berlin, 2010, pp. 267–315, Chapter 7.
11. G. Adamian, N. Antonenko, W. Scheid, in: C. Beck (Ed.), *Clusters in Nuclei*, vol. 2, in: *Lect. Notes Phys.*, vol. 848, Springer-Verlag, Heidelberg, Berlin, 2012, pp. 165–227.
12. D. Poenaru, W. Greiner, in: C. Beck (Ed.), *Clusters in Nuclei*, vol. 1, in: *Lect. Notes Phys.*, vol. 875, Springer-Verlag, Berlin, Heidelberg, 2010, pp. 1–56.
13. Yu.V. Pyatkov, et al., *Eur. Phys. J. A* 45 (2010) 29.
14. Yu.V. Pyatkov, et al., *Eur. Phys. J. A* 48 (2012) 94.
15. W. von Oertzen, Y.V. Pyatkov, D. Kamanin, in: *Zakopane Conference*, *Acta Phys. Pol.* 44 (2013) 447.
16. M. Csatlos, A. Krasnahorkay, P.G. Thirolf, et al., *Phys. Lett. B* 615 (2005) 213.
17. K.R. Vijayaraghavan, W. von Oertzen, M. Balasubramaniam, *Eur. Phys. J. A* 48 (2012) 27.
18. W. von Oertzen, A.K. Nasirov, *Eur. Phys. J. A* 47 (2011) 136.
19. P. Schall, et al., *Phys. Lett. B* 191 (1987) 339.

20. K. Assamagan, et al., Time-zero fission-fragment detector based on low-pressure multi-wire proportional chambers, Nucl. Instr. and Meth. A 426 (1999) 405-419.
21. A. Margaryan, et al., Low-pressure MWPC system for the detection of alpha-particles and fission fragments. Armenian Journal of Physics, (2010) vol. 3, issue 4, 282-291.
22. A. T. Margaryan et al., Journal of Contemporary Physics, Vol. 54, No. 2, p. 117 (2019).

Appendix 7

Heavy Ion Radio Frequency Timer: A Picosecond Resolution Heavy Ion Detector for Nuclear Physics Applications

S. Abrahamyan¹, R. Ayvazyan¹, G. Ayvazyan¹, J. R. M. Annand², D. L. Balabanski³, N. Demekhina¹, H. Elbakyan¹, B. Grigoryan¹, N. Grigoryan¹, V. Kakoyan¹, P. Khachatryan¹, V. Khachatryan¹, K. Livingston², S. Mailyan¹, R. Montgomery², S. N. Nakamura⁴, J. Pochodzalla⁵, H. Vardanyan¹, S. Zhamkochyan¹, A. Margaryan¹

1. A.I. Alikhanyan National Science Laboratory
2. School of Physics & Astronomy, University of Glasgow
3. ELI-NP, Bucharest 077125, Magurele, Romania
4. Tohoku University, Sendai, Japan
5. Johannes Gutenberg Universitat, Mainz, Germany

An ultra-high time resolution heavy ion detector for applications in nuclear physics is under development at the AANL. The principle of operation of the device based on a radio frequency (RF) ps-resolution timing processor of keV electrons is outlined. Possible applications to fission isomer studies on the proton and photon beams of the cyclotron C18/18 and ELI-NP, Magurele, Bucharest and in the hypernuclear studies on the 1.5 GeV electron beam of MAMI, Mainz are discussed.

RF timer for keV electrons

A new ps-resolution RF timing processor for keV electrons [1, 2] is under development at the AANL in the framework of the ISTC A-2390 project. An ultra-high time resolution heavy ion detector based on this new timing processor is under development. The principle of operation of this detector is schematically shown in Fig. 1. The primary beam hits the target (1) and produces secondary electrons (SE) and reaction products, e.g. prompt or delayed fission fragments (FF). The FF exiting from the target produces a few tens of SEs. These electrons are accelerated by a voltage V applied between the target and an electron transparent electrode (2) up to energies of a few keV. They are deflected by the magnet (3), pass through the collimator (4) and enter the electrostatic lens (5). The lens then focuses electrons onto the screen (10) at the far end of the tube, where the high-resolution electron detector is placed. Along the way, the

electrons pass through the circular sweep RF deflection system consisting of electrodes (6) and RF tuning system (7), which operates at frequencies of 500-1000 MHz. They are deflected (8, 9) to form a circle or a spiral on the screen (10). A different type of position readout technique can be used. A pixel-by-pixel readout anode with a resolution of $55\ \mu\text{m}$ will permit counting rates much higher than MHz [3, 4]. The overall time resolution of this timing technique is about a few ps [5], and the expected time drift is 1-2 ps/hrs [6].

Spiral scanning will increase the pico-time period. Two helical deflectors at slightly different RF frequencies produce a “beat” in the amplitude of the scanned circle which sets the period for a single pico-time spiral sequence. Adding a pixelated anode, the RF Timer becomes a self-contained, single-electron timer with ps resolution. Each pixel is a separate ps time gated counter and can be used as a trigger for delayed events in a ps-ns time domain. This provides new opportunities for nuclear and hypernuclear studies at modern electron-proton accelerators.

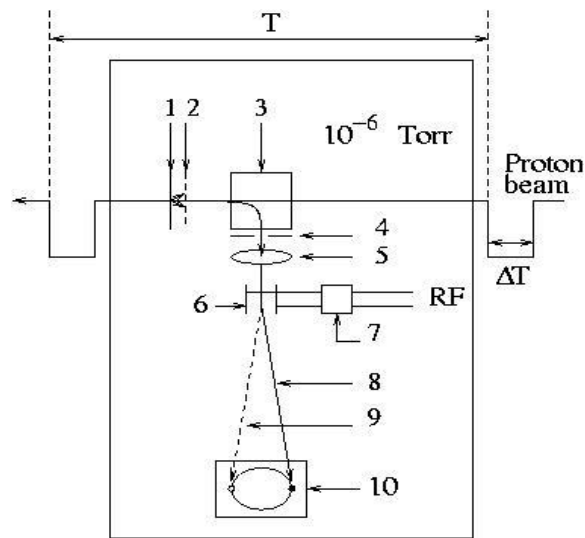


Fig. 1: Schematic of the heavy ion radiofrequency timer (see text for details)

Study of fission isomers on the RF synchronized pulsed proton beams

The ground state of an atomic nucleus corresponds to the minimum in the potential energy surface (PES). In some nuclei, there exist two minima which correspond to two wells in PES, (see Fig. 2).

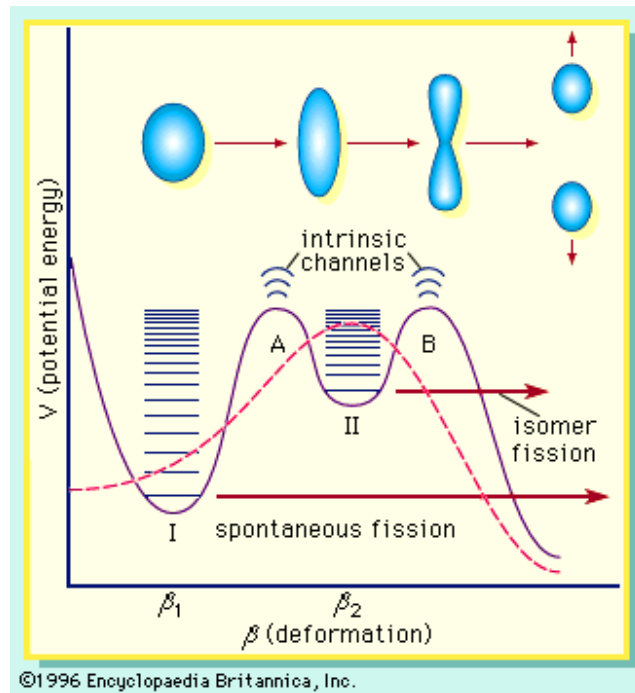


Fig. 2: Schematic illustrations of single-humped and double-humped fission barriers. The former is represented by the dashed line and the latter by the continuous line. Intrinsic excitations in the first and second wells at deformations β_1 and β_2 are designated class I and class II states, respectively. Intrinsic channels at the two barriers also are illustrated. The transition in the shape of the nucleus as a function of deformation is schematically represented in the upper part of the figure. Spontaneous fission of the ground state and isomeric state occurs from the lowest energy class I and class II states, respectively.

Metastable state exists in the second well of PES. In the actinide mass region ($Z > 90$), the metastable state is often termed “fission isomer”, since most of the fission isomers decay by spontaneous fission (SF). Fission isomers in the actinide region were observed by Polikanov et al. [7] as early as in 1962. In a few years, for the first time, Strutinsky [8] described that state by a macroscopic-microscopic method. At fission shapes where shell gap exists, the special shell structure of single-particle orbits leads to the appearance of the second minimum in PES. Because of the significant barrier between the first and second minima, the decay from the fission isomer to the ground state is highly inhibited. The fission isomers of actinide nuclei have extremely elongated shapes (major-to-minor axis ratios of approximately 2:1). Later, the existence of a third PES minimum (major-to-minor axis ratio of approximately 3:1) was suggested in theory and experiment [9]. Recently, the observed γ spectroscopy and transmission resonances have provided more information about the states in the second and third wells [10]. Fission isomers have been discovered in 34 actinide nuclei (such as $^{236,238}\text{U}$, $^{236,238,240,242}\text{Pu}$ and $^{240,242,244}\text{Cm}$ [10, 11]). However, only half lives and excitation energy has been measured for most fission isomers [11]. Thus far, we have obtained quite limited details about transition energies only in $^{236,238}\text{U}$ and ^{240}Pu fission isomers [10-16]. Many properties of other fission isomers of nuclei have not been determined as a result of the lack of experimental investigations [17]. Therefore, there is a great need in further experimental observations.

In reactor physics, detailed information of fission isomers in actinide is helpful for understanding the fuel fabrication process. The properties of fission isomers may promote the progress in the astrophysical science. The accurate data of fission states are useful for

understanding of nuclear syntheses in the core of stars [18]. With the data, we can estimate the age of the Galaxy with the nuclear chronometers, as long-lived heavy elements are formed mostly in the r-process irradiation [19].

The life-times of the fission isomers in a ps-ns range can be measured precisely by using the heavy ion RF timer at pulsed proton and photon beams. The delayed decay of the shape isomer provides a unique experimental tag to identify the class II states in the second well of PES. The heavy ion detector with a pixelated anode allows to carry out time-gated spectroscopy of these states as well as to study the exotic decay channels of fission isomers (such as ternary fission phenomena) on the RF synchronized pulsed proton and photon beams of Yerevan cyclotron and at the laser Compton backscattered facility, ELI-NP, Magurele, Bucharest.

Outlook

The prototype version of the RF timer (Fig. 4) is currently under evaluation at AANL and we expect further field trials at the CANDLE fast pulse facility in Yerevan. Already the delay-line readout from the circular scanning system and the first dual-deflector spiral-scanning systems are being tested. Ready prototypes will be tested at the proton cyclotron C18/18, Mainz Microtron facility in Germany, ELI-NP photon beams in Bucharest, Romania and at the ELPH internal electron beam, Tohoku University, Japan. The ps timing resolution of the RF timer is by a factor of up to 100 better than that of the regular timing technique. The RF timer can be operated synchronously with RF driven particle bunches and is ideally suited to time measurement applications in nuclear and high energy physics experiments.

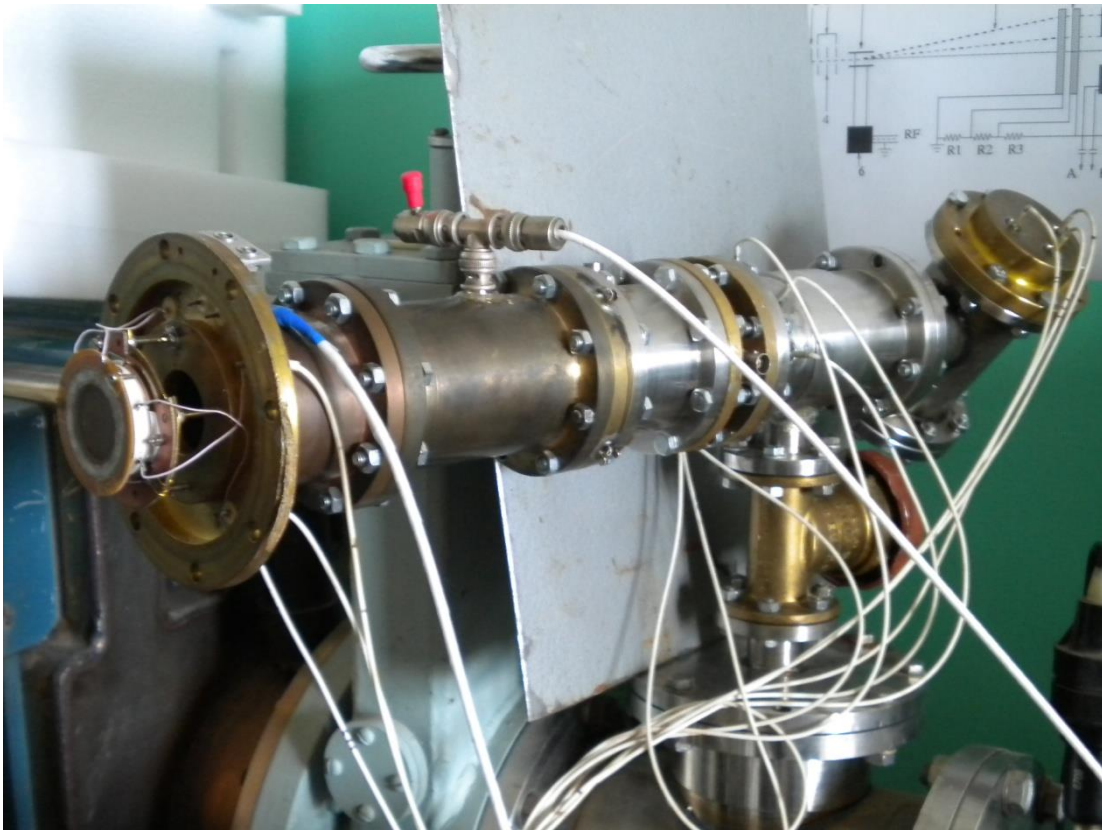


Fig. 4: General view of the heavy-ion radiofrequency timer

References

1. Margarayn et al., Nucl. Instr. and Meth. A 566 (2006), 321.
2. L. Gevorgian, et al., Nucl. Instr. and Meth. A785 (2015), 175.
3. A. Margaryan, et al., Single Photon THz Timer with Radio Frequency PhotoMultiplier Tube, Proc. PhotoDet2012, 13-15 June 2012, Orsay, LAL, Paris, France, Proceedings of Science, <http://pos.sissa.it>.
4. J. Vallerga et al., Journal of Instrumentation, (2014) 9, C05055.
5. A. Margaryan, et al., Bunch time structure detector with picosecond resolution, Vasili Tzakanov and Helmut Wiedemann (eds), Brilliant Light in Life and Material Sciences, 455, Springer (2007).
6. K. Scheidt. Proceedings of EPAC 2000, Vienna, Austria, (2000) p. 182.
7. Polikhanov S M, Druin V A, Karnaukhov V A, et al. Spontaneous fission with an anomalously short period. Sov Phys JETP, 1962, 15: 1016–1022; Polikanov S M, Druin V A, Karnaukhov V A, et al. Spontaneous fission with an anomalously short half-life. Zhur Eksptl Teoret Fiz, 1962, 42: 1464–1471.
8. Strutinsky V M. Shell effects in nuclear masses and deformation energies. Nucl Phys A, 1967, A95: 420–442.
9. Blons J. A 3rd minimum in the fission barrier. Nucl Phys A, 1989, 502: c121–c140.
10. Thirolf P G, Habs D. Spectroscopy in the second and third minimum of actinide nuclei. Prog Part Nucl Phys, 2002, 49: 325–402.
11. Singh B, Zywina R, Firestone R B. Nucl Data Sheets 2002, 97: 241. Evaluated Nuclear Structure Data File, <http://www.nndc.bnl.gov/ensdf/>
12. Schirmer J, Gerl J, Habs D, et al. Gamma-decay of the superdeformed shape isomer in U-236. Phys Rev Lett, 1989, 63: 2196–2199.
13. Thirolf P G. Perspectives for spectroscopy of actinides with highly brilliant gamma beams. Acta Phys Pol B, 2012, 43: 227–232.
14. Singh B, Firestone R B, Frank Chu S Y. Table of Superdeformed Nuclear Bands and Fission Isomers. 2nd ed. Wiley Interscience, 1996.
15. Pansegrau D, Reiter P, Schwalm D, et al. Gamma spectroscopy in the superdeformed minimum of Pu-240. Phys Lett B, 2000, 484, 1: 1–9.
16. Gassmann D, Thirolf P G, Mergel E, et al. Conversion electron spectroscopy in the superdeformed minimum of Pu-240. Phys Lett B, 2001, 497, 3-4: 181–189.
17. Rauscher T, Heger A, Hoffman R D, et al. Nucleosynthesis in massive stars with improved nuclear and stellar physics. Astrophys J, 2002, 576: 323–348
18. Truran J W. The age of universe from nuclear chronometers. Proc Nat Acad Sci USA, 1998, 95: 18–21.
19. Xie K P, Ke W Y, Liang W Y, et al. Collective rotations of fission isomers in actinide nuclei. Sci China-Phys Mech Astron, 2014, doi: 10.1007/s11433-013-5379-8.

Appendix 8

Search for emission π^0 -meson emission in proton-induced fission of uranium

A.Aleksanyan, S.Amirkhanyan, H. Gulkanyan, T.Kotanjyan, V.Pogosov, O.Pogosova,
L.Poghosyan

The energy released in the spontaneous fission of heavy nuclei is about 200 MeV. It is not forbidden, that a part of this energy can be spent for the production of a pion – process called pion radioactivity [1] (see [2] for review on this and other forms of the exotic radioactivity). In recent studies of the ^{252}Cf spontaneous fission, an indication was obtained (however, not yet confirmed) on the registration of light charged particles (presumably π^\pm or μ^\pm) [3]. In the spontaneous fission of ^{257}Fm , the upper limits for the emission of charged pions were stated: $(1.2 \pm 0.2) \cdot 10^{-3} \pi^-$ /fission [4] and $(7 \pm 6) \cdot 10^{-3} \pi^+$ /fission [5]. A much more severe restriction was obtained [6] for the π^0 -emission in the spontaneous fission of ^{252}Cf : $< 3 \cdot 10^{-13}$ /fission, a value close to the theoretical prediction [7].

For the case of induced fission which proceeds via higher excited intermediate states, the probability of the exotic radioactivity is expected to be much higher respective to the spontaneous fission case [8]. To date, the strongest experimental restriction on the π^0 -emission was obtained in the thermal neutron-induced fission of ^{235}U and amounts less than $5.3 \cdot 10^{-12}$ /fission [9].

We suggest searching for the π^0 -emission in proton-induced fission of ^{238}U . The decay gammas with energies of about 67.5 MeV and opening angle close to 180° will be searched for by using a set of NaI(Tl) scintillation detectors enable to decrease the limit on the π^0 - emission in the proton-induced fission of ^{238}U up to the level better than $5 \cdot 10^{-13}$ /fission.

References

- [1] D.B. Ion, M. Ivascu, R. Ion-Mihai, Ann. Phys. (N. Y) 171 (1986) 237
- [2] D.B. Ion, R. Ion-Mihai, M.L. Ion, arXiv: 0710.0744, 12 Jan 2013
- [3] V.A. Khryachkov et al., Instr. Exp. Tech. 45 (2002) 615
- [4] D.B. Ion, R. Ion-Mihai, D. Bucurescu, Rev. Roum. Phys. 34 (1989) 261
- [5] K. Janko, P. Povinec, Proc. 14-th Europhys. Conf., Rare Nuclear Processes, Bratislava, 22-26 October 1990, (Ed. P. Provinec), p.121
- [6] V. Bellini et al., Proc. 14-th Europhys. Conf., Rare Nuclear Processes, Bratislava, 22-26 October 1990, (Ed. P. Provinec), p.116
- [7] D.B. Ion, R. Ion-Mihai, M. Ivascu, Rev. Roum. Phys. 33 (1988) 1071
- [8] A.S. Iljinov, M.V. Mebel, Phys. Atom. Nucl. 64 (2001) 1368
- [9] V.A. Varlachev et al., JETP Letters 80 (2004) 149

Appendix 9

Formation of neutron beams

R.Avetisyan, A.Barseghyan, Yu.Gharibyan, A.Gyurjinyan, I.Kerobyan, H.Mkrtchyan, V.Yaralov

The cyclotron C18/18 produces proton beam with energy 18 MeV and current up to 100 μA . On the base of external proton beam of C18/18 formation of the neutron beam is planned. The obtained neutron beams will be used for investigation the neutron-induced reactions as well as for applied problems.

The modified C18/18 has a special vacuum pipe for passing protons. Before bombarding the target proton beam pass through the 500 μm foil from Al which is installed for keeping the vacuum inside the tube. After passing through the Al foil protons lose part of the energy from 18 MeV to 14.8 MeV.

To obtain a high neutron yield two materials were used commonly. That materials are ^7Li and ^9Be . There is substantial difference in the melting temperature of Li and Be. For ^9Be (1287°C) the melting point is much higher than for ^7Li (180.54°C), that's why ^9Be as target was chosen [1].

First of all the optimal thickness of the target for obtaining of higher yield of neutrons was determined. To obtain the energy spectra of neutrons for 0.5 mm, 1 mm and 2.5 mm thicknesses of Be target at proton beam energy 14.8 MeV the simulation by GEANT4 [2] was performed.

The neutron yield growth in dependence of Be target thickness is observed (Figure 1). To produce neutron beams an optimal thickness of the target ^9Be thickness of 2.5 mm was chosen, for which further calculations were performed.

The obtained neutron fluxes are accompanied by the high intensity of gamma rays. The effective way for getting more neutrons than gamma rays after the target system (beryllium target with lead plate) is the using of 2.5 mm Be and 1.27 cm lead plate [3].

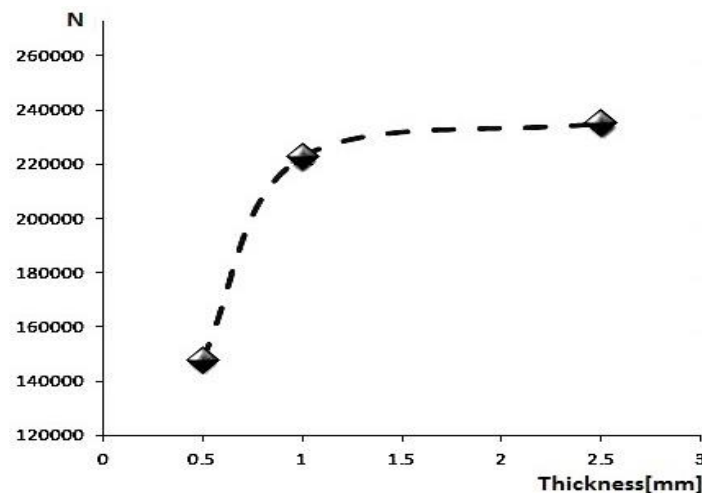


Fig. 1. Yield of neutrons in dependence of the thicknesses of Be

To design of the neutron beam formation system, GEANT4 simulation was performed. As a result of simulations the effective materials and sizes of Beam Shaped Assembly (BSA) [4] were determined (Figure 2). To increase neutrons by the reaction (n,2n) the system should include bismuth. The optimal thickness of the bismuth sheet is 5 cm.

For low energy neutron beam formation, appropriate BSA with the moderator and reflector was simulated by GEANT4 program. The system consists of 5 cm bismuth for (n,2n) reactions, 50 cm iron, 10 cm aluminum and 5 cm graphite as moderators and lead as reflector [5]. After using this system the energy of neutrons will be lowered from 13 MeV to 1 MeV. Future GEANT4 simulations needed for getting thermal and epithermal neutrons.

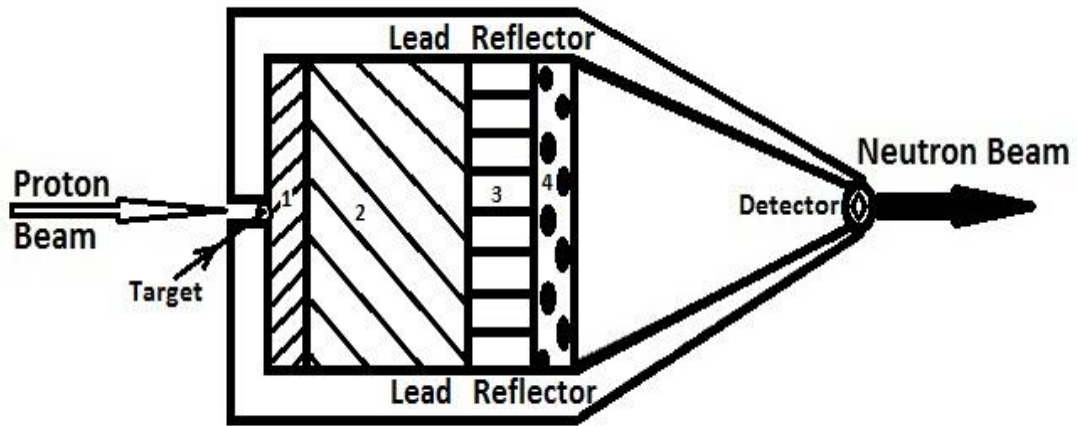


Fig. 2. System consists of 2.5 mm Be target, 5cm Bi (1), moderator from 50 cm Fe (2), 10 cm Al (3) and 5cm graphite (4), lead reflector and detector

The neutron detector with radius 5 cm will be connected to conical reflector. The simulation was performed for different materials and different thicknesses of the reflectors to determine their reflective capabilities. Thin layers of lead will be used at the end of moderation to decrease the undesirable photon dose.

In Figure 3 the results of the simulation for low energy neutron beam formation are presented. A mainly detected neutron has energies less than 1 MeV and it is important to get higher count of neutrons with very low energies. In the region of energy up to 200 keV the neutron beam intensity about $1.4 \cdot 10^7$ n/s*cm² will be achieved for 100 μ A proton current.

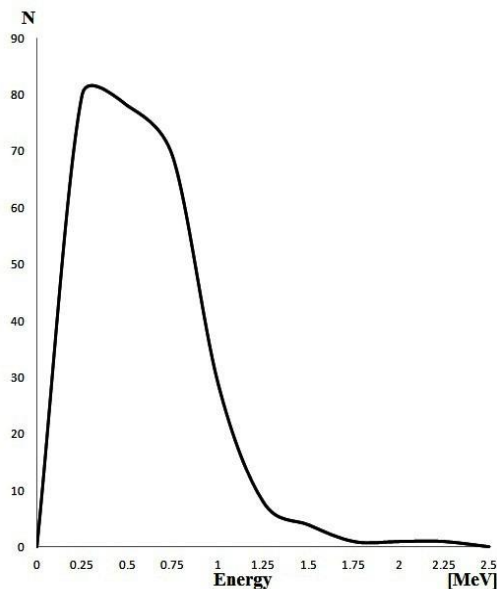


Fig. 3. Energy spectra of low energy neutron beam detected after the system of moderator and reflector

It is planned to continue further work on improving the BSA in order to obtain thermal-epithermal neutrons suitable for use in BNCT.

References

1. R. Avagyan, R. Avetisyan, V. Ivanyan, I. Kerobyan “Study of low energy neutron beam formation based on GEANT4 simulations” Nuclear Instruments and Methods in Physics Research B 402 (2017) 247–250.
2. <https://geant4.web.cern.ch/geant4/>
3. . R. Avagyan, R. Avetisyan, V. Ivanyan, I. Kerobyan: GEANT4 Simulations of a Beam Shaping Assembly Design and Optimization for Thermal/Epithermal Neutrons; January 2017, Acta Physica Polonica Series B 48(10):1693.
4. Jerome M. Verbeke, Allen S. Chen, Jasmina L. Vujic, Ka-Ngo Leung “Optimization of Beam-Shaping Assemblies for BNCS Using the High-Energy Neutron Sources D-D and D-T”, Nuclear Technology, Vol. 134, June 2001
5. Daniel R. McAlister, PhD “Gamma Ray Attenuation Properties of Common Shielding Materials”, PG Research Foundation, Inc. 1955 University Lane Lisle, IL 60532, USA.

Appendix 10

Neutron-Deuteron Scattering in the Energy Range from 100 keV to 5 MeV

S. Abrahamyan, R. Ayvazyan, N. Demekhina, H. Elbakyan, N. Grigoryan, H. Jilavyan, V. Kakoyan, P. Khachatryan, V. Khachatryan, H. Vardanyan, S. Zhamkochyan, A. Margaryan

Neutron-deuteron scattering is one of the most fundamental interaction processes in a few-body quantum system. Besides understanding quantum mechanical few-body systems, the differential neutron-deuteron (n-d) scattering cross section is also relevant for nuclear technology, and nuclear astrophysics. The inconsistencies of the available experimental data have prompted the inclusion of the differential neutron-deuteron scattering cross section in the OECD high-priority request list (HPRL) [8] for urgent nuclear data measurements. We propose an experimental program for a detailed study of n-d scattering with the help of the recently developed Low-Energy Nuclear Interaction Chamber (LERNIC) and fission neutrons from 18 MeV proton ^{238}U interactions at the cyclotron C18/18.

Next to the neutron-proton (n-p) scattering ($N = 2$), the neutron-deuteron scattering ($N = 3$) is the most fundamental interaction process in a few-body quantum system consisting of N nucleons. It can be described by the re-formulated Fadeev three-body equations [1], using the well-developed nucleon-nucleon potentials for the interaction between the three nucleons involved. These calculations covered the energy range from 3 MeV to 19 MeV which was later extended to a lower limit of 50 keV [2].

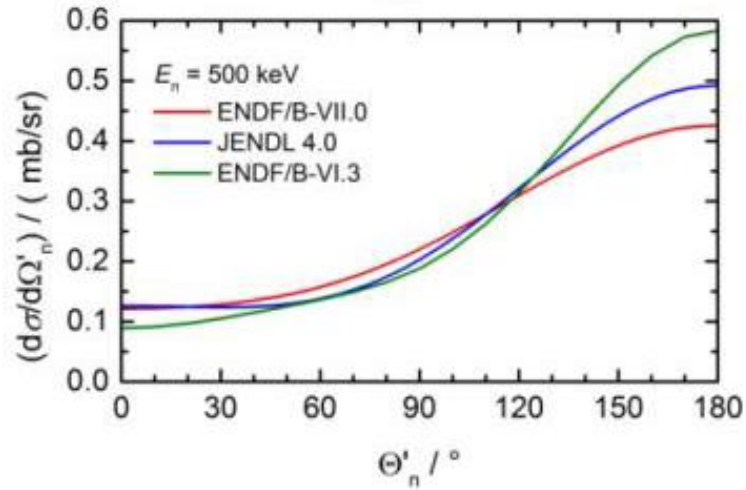


Fig. 1: The angular distributions of 500 keV neutrons in the CM system from ENDF/B-VII.0 (red line), JENDL 4.0 (blue line) and ENDF/B-VI.3 (green line). The calculations were fitted to the experimental data in the recoil energy range above 120 keV, corresponding to a neutron-deuteron scattering angle of $\Theta'_n = 117.3^\circ$. Data is taken from Ref. [3].

In addition to its relevance for understanding quantum mechanical few-body systems, the differential neutron-deuteron (n-d) scattering cross section is also relevant for nuclear technology, in particular for the design and safe operation of heavy-water moderated reactors. Several critical and subcritical benchmark experiments for heavy-water moderated configurations demonstrated the sensitivity of the effective neutron multiplication factor k_{eff} and the coolant void reactivity (CVR) to the angular distribution of the neutron-deuteron scattering cross sections [4]. In particular, significant changes in the calculated k_{eff} and CVR values were observed when the data of the ENDF/B-VI.3 [5] library were replaced by the data from later releases.

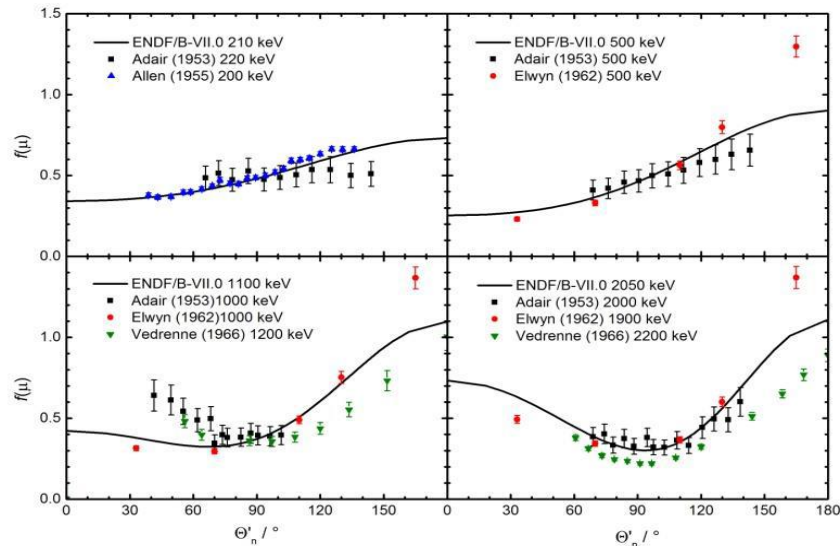


Fig. 2: Experimental angular distributions (symbols) for neutron-deuteron scattering for the energy range from 100 keV to 2000 keV compared with evaluated angular distributions from ENDF/B-VII.0 (solid lines) calculated for the mean neutron energy of the data sets. Data is taken from Ref. [3].

It is very striking to see that the experimental data base supporting the evaluations is rather scarce and partially inconsistent, with some of the measurements dating back to the 1950's and 1960's. As an example, Fig. 2, taken from Ref. [3], shows the experimental data available from EXFOR [6] for the energy range from 100 keV to 2 MeV. The data are grouped into four narrow energy intervals and compared with the angular distributions from ENDF/B-VII.0 [7] calculated for the mean energy of each energy interval. The inconsistencies of the available experimental data and, in particular, the difficulty of reproducing the results of benchmark experiments have prompted the inclusion of the differential neutron-deuteron scattering cross section in the OECD high-priority request list (HPRL) [8] for urgent nuclear data measurements.

We propose an experimental program for a detailed study of (n,p), (n,d), (n,³He) and (n,⁴He) reactions in the neutron energy range from 100 keV to 5 MeV, by using the Low Energy Nuclear Interaction Chamber (LERNIC) recently developed at AANL [9] (see Fig. 3).

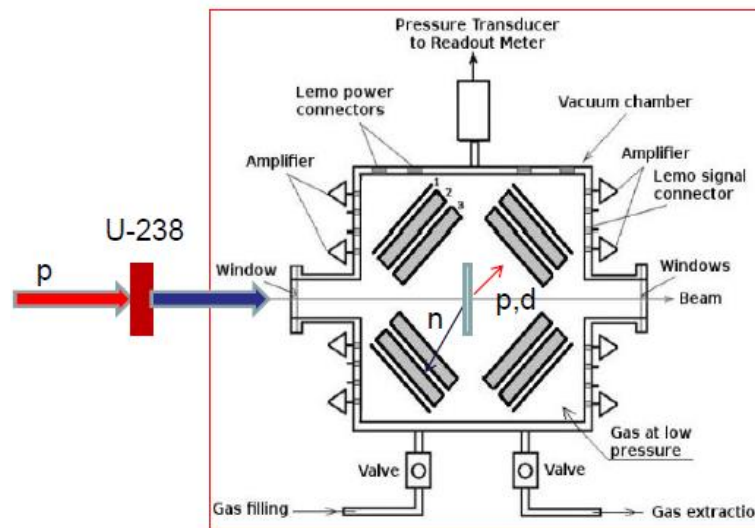


Fig. 3. Schematic of the low-energy nuclear interaction chamber.

The neutrons will be produced at the proton-induced fission of ²³⁸U. The expected neutron spectra will be similar to those from ²⁴²Pu(p,f) [10], the experimental and theoretical results of which for $E_p = 20$ MeV are presented in Fig. 4.

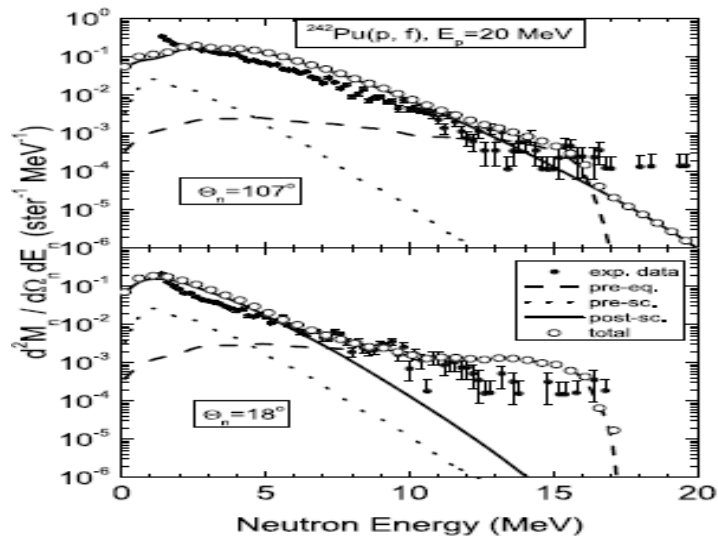


Fig. 4. Experimental (points with error bars) and theoretical (circles) fission prompt neutron spectra in ^{242}Pu (p,f) at $E_p=20$ MeV at laboratory frame angles of 18° and 107° in coincidence with the fission fragment detectors placed at an angle of about 88° . Data is taken from Ref. [10].

The energy resolution of the recoils (proton, deuteron, helium) in the energy range of few hundred keV will be determined by ToF in LERNIC and is expected to be about 10%. The recoil angles will be determined with an accuracy of about few degrees. The neutron energy will be determined from two-body kinematics and is expected to be about 10%.

References

1. L. Canton, W. Schadow, and J. Haidenbauer, *Eur. Phys. J. A* **14** (2002) 225
2. J.P. Svenne, L. Canton, K. Kozier, and L. Townsend, *Proc. International Conference on Nuclear Data for Science and Technology 2007, Nice, April 22-27, 2007*, DOI 10.1051/ndata:07208
3. R. Nolte et al., *ERINDA 2013 Workshop Proceedings* p. 187-195, <http://publications.jrc.ec.europa.eu/repository/handle/JRC88201>
4. K.S. Kozier, *Proc. International Conference on Nuclear Data for Science and Technology 2007, Nice, April 22-27, 2007*, DOI 10.1051/ndata:07594
5. P.G. Young, *n + D Evaluation to 100 MeV, Release 3, ENDF/B-VI evaluation*, distributed April, 1995
6. *Experimental Nuclear Reaction Data (EXFOR)*, available online: <https://www.nds.iaea.org/exfor/exfor.htm>
7. M.B. Chadwick *et al.*, *Nucl. Data Sheets* **107** (2006) 2931
8. *NEA Nuclear Data High-Priority Request List*, available online: <http://www.oecdnea.org/dbdata/hprl/>
9. A. T. Margaryan et al., *Journal of Contemporary Physics*, Vol. 54, No. 2, p. 117 (2019).
10. V. A. Rubchenya, *Phys. Rev. C* **75**, 054601(2007)